Chemosphere 365 (2024) 143318

Contents lists available at ScienceDirect

Chemosphere

journal homepage: www.elsevier.com/locate/chemosphere

Antifouling activity and ecotoxicological profile of the cyanobacterial oxadiazine nocuolin A

Sandra Pereira [a,b], Isabel B. Oliveira [a], Maria Lígia Sousa [a], Catarina Gonçalves [a,b], Marco Preto [a], Maria V. Turkina [c], Vitor Vasconcelos [a,b], Alexandre Campos [a], Joana R. Almeida [a,*]

[a] CIIMAR- Interdisciplinary Centre of Marine and Environmental Research, University of Porto, Terminal de Cruzeiros do Porto de Leixões, Avenida General Norton de Matos, s/n, 4450-208, Matosinhos, Portugal
[b] Biology Department, Faculty of Sciences, University of Porto, Rua do Campo Alegre, 4169-007, Porto, Portugal
[c] Department of Biomedical and Clinical Sciences, Faculty of Medicine and Clinical Sciences, Linköping University, 581 83, Linköping, Sweden

HIGHLIGHTS

- The cyanobacterial natural oxadiazine nocuolin A exhibits antifouling activity.
- Nocuolin A is effective against the settlement of mussel plantigrades and the growth of marine diatoms.
- Nocuolin A affects target proteins involved in muscle regulation, ER stress, and ATP production in mussels.
- Ecotoxicological effects were observed for *Navicula* sp., Artemia salina, *Amphibalanus amphitrite*, and *Danio rerio*.
- The reported ecotoxicity hinders the potential of nocuolin A as an antifouling agent.

GRAPHICAL ABSTRACT

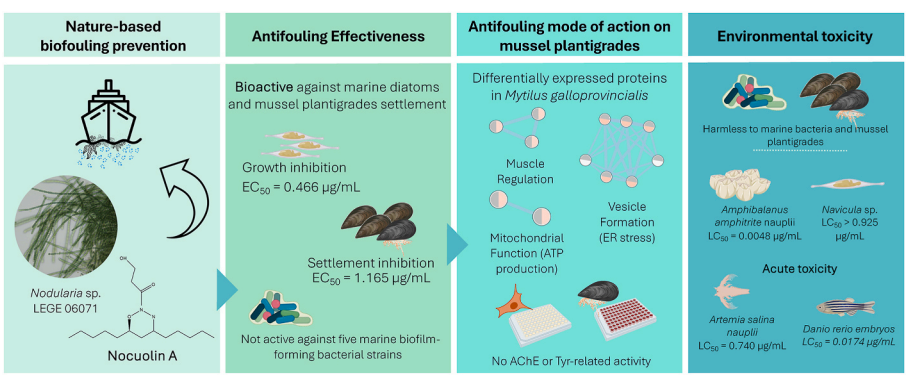

ARTICLE INFO

Handling editor: James Lazorchak

Keywords:
Biofouling
Antifouling
Natural products
Cyanobacteria
Nocuolin A
Environmental compatibility

ABSTRACT

Pursuing effective and biocompatible natural compounds to supplant current biocidal antifouling (AF) technologies remains crucial and challenging. Among natural products hosts, cyanobacteria are recognized as producers of bioactive secondary metabolites that are underexplored in terms of anti-biofilm and AF potential. Nocuolin A, a natural oxadiazine previously isolated and known to be produced by different cyanobacterial strains, has demonstrated bioactive potential, particularly against tumor cell lines. Considering this potential and its exquisite chemical structure, here nocuolin A was investigated as a potential natural AF agent through an integrative approach including AF bioactivity testing across distinct levels of biological organization, mode of action assessment, ecotoxicity evaluation, and ecological risk predictions. Nocuolin A was found to inhibit the settlement of mussel (*Mytilus galloprovincialis*) plantigrades (EC_{50} = 3.905 μM) while showing no toxicity to this biofouling species (LC_{50} > 100 μM). Additionally, while exhibiting no inhibitory activity against the growth of

* Corresponding author.CIIMAR | Interdisciplinary Centre of Marine and Environmental Research of the University of Porto Terminal de Cruzeiros do Porto de Leixões, Avenida General Norton de Matos, S/N, 4450-208 Matosinhos, Portugal.

E-mail addresses: sandra.pereira@ciimar.up.pt (S. Pereira), isabel_s_oliveira@yahoo.com (I.B. Oliveira), ligiasilvasousa@gmail.com (M.L. Sousa), catarinaisgoncalves22@gmail.com (C. Gonçalves), mcpreto@gmail.com (M. Preto), maria.turkina@liu.se (M.V. Turkina), vmvascon@fc.up.pt (V. Vasconcelos), amoclclix@gmail.com (A. Campos), jalmeida@ciimar.up.pt (J.R. Almeida).

https://doi.org/10.1016/j.chemosphere.2024.143318
Received 3 August 2024; Received in revised form 8 September 2024; Accepted 10 September 2024
Available online 11 September 2024

five marine biofilm-forming bacterial strains, it significantly suppressed the growth of the marine biofilm-forming diatom *Navicula* sp. (EC_{50} = 1.561 μM), and had a lethal effect on this diatom species (>3.1 μM). The AF targets of nocuolin A on mussel plantigrades revealed no correlation with acetylcholinesterase and tyrosinase metabolic processes; however, proteins involved in oxidative stress, muscle regulation, and energy production were highlighted. The results also provide insights into the ecological risk of nocuolin A, including its ecotoxicity against *Artemia salina* nauplii (LC_{50} = 2.480 μM), *Amphibalanus amphitrite* nauplii (LC_{50} = 0.0162 μM), and *Danio rerio* embryos (LC_{50} = 0.0584 μM). When matching these results with simulated environmental values, nocuolin A was deemed a considerable threat to the ecosystems. While this research highlights the AF activity of nocuolin A, it also emphasizes the potential adverse environmental impact when applied in preventive coatings.

1. Introduction

Marine biofouling is the natural process that occurs on all submerged surfaces, characterized by the rapid colonization of organic molecules, and successively a micro and macro biological community. This biological colonization leads to serious problems and requires large investments for the maritime industries, as well as raising environmental concerns due to the antifouling (AF) biocidal agents currently in use as components of marine coatings (Paz-Villarraga et al., 2022; Schultz et al., 2011; Yebra et al., 2004). In compliance with recent EU strategies for sustainability, new effective and environmentally compatible alternatives to biofouling control are needed (European Commission & European Climate Infrastructure and Environment Executive Agency, 2021). Natural products are believed to have the potential to provide solutions for a wide range of biotechnological applications, including AF, which could be effective and ecologically compatible. Following this premise, several natural antifoulants have been described so far from both terrestrial and marine sources (Pereira et al., 2024), however, their environmental impact is often overlooked based on the assumption that they are derived from natural sources.

Among the natural sources, cyanobacteria, a biodiverse group of photosynthetic prokaryotes, are known to produce a variety of chemically diverse secondary metabolites, encouraging further investment in the bioprospection of this particular group for AF bioactive compounds (Antunes et al., 2019; Brown et al., 2004; Dahms et al., 2006; Tan et al., 2010). In addition, a better understanding of natural products' AF mode of action and ecotoxicity profile remains necessary, keeping some promising compounds far from being considered for commercial purposes. Among the cyanobacterial-derived compounds discovered so far, nocuolin A, a natural oxadiazine, was originally isolated from the cyanobacterium *Nostoc* sp. CCAP1453/38 and is notable for its unique structure with a six-membered 1,2,3-oxadiazine heterocycle (Fig. 1), exhibiting pro-apoptotic properties and a potent antiproliferative activity (0.7–4.5 μM) against several human cancer lines (Voráčová et al., 2017). The compound was later found in three independent cyanobacterial strains of genera *Nostoc*, *Nodularia*, and *Anabaena,* all of which have the enzymes of the *noc* biosynthetic gene cluster for nocuolin A biosynthesis in their genomes (Voráčová et al., 2017; Martins et al., 2022). The antiproliferative effect of the compound was further investigated and associated with the weakening of mitochondrial oxidative phosphorylation followed by cell autophagy, after nocuolin A isolation from a cyanobacterial strain *Nodularia* sp. LEGE 06071 (Sousa et al., 2019).

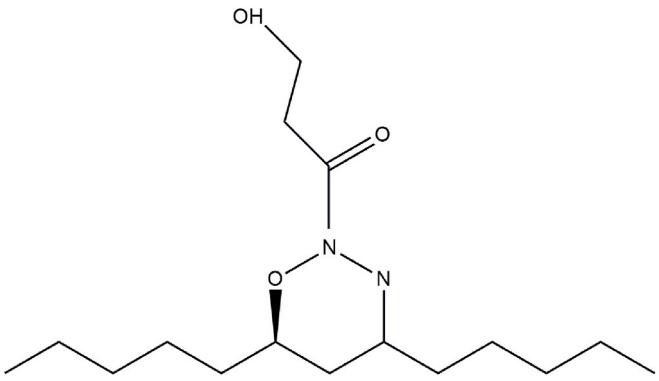

Fig. 1. Cyanobacteria-derived compound nocuolin A.

Considering its uniqueness and biotechnological potential, recent studies have been conducted on nocuolin A, including optimization of production parameters (Chmelík et al., 2019), pursuing its natural biosynthetic pathways (Martins et al., 2022), the discovery of new nocuolin A hybrids (Figueiredo et al., 2021), and the synthesis of new nocuolin A semisynthetic analogues (Pérez et al., 2023). However, the investigation of nocuolin A as a promising biotechnological tool for applications targeting unrelated molecular pathways, such as AF activity, remains unexplored. In light of this, here we aim to unveil nocuolin A's overall potential for use in environmentally compatible biofouling preventive systems, through an integrative approach testing AF efficiency, putative AF molecular targets, and predicted marine ecotoxicity. Antifouling efficiency was evaluated against representative micro and macrofouling organisms. In addition, the elucidation of molecular targets underlying the AF activity observed in mussel plantigrades was performed, as the understanding of the mechanisms of action associated with AF compounds remains a research challenge. Since biofouling is a complex phenomenon involving a wide range of different organisms, AF compounds are believed to affect colonization/settlement through distinct pathways (Almeida and Vasconcelos, 2015; Chen and Qian, 2017). Considering this, *in vitro* tyrosinase and acetylcholinesterase (AChE) enzymatic assays, were performed in the presence of nocuolin A, and a whole organism-untargeted shotgun proteomic approach was used with mussel plantigrades after exposure to nocuolin A, to assess the most prominent proteins affected. Finally, the environmental toxicity of nocuolin A was investigated in different organisms using lethal and sub-lethal endpoints and *in silico* predictions. The observed multi-organism interactions provided insights into the potential ecological function of nocuolin A within its native cyanobacterial hosts. As seen in other studies on AF compounds (Oliveira et al., 2014, 2017; Wang et al., 2014), the information generated in this study was also used, together with predicted environmental concentration, as a proxy for nocuolin A's putative ecological risk.

2. Material and methods

2.1. Nocuolin A isolation

Nocuolin A was obtained following the method described by Sousa et al. (2019), with minor adjustments. Briefly, the cyanobacterial strain *Nodularia* sp. LEGE 06071, from the Blue Biotechnology and Ecotoxicology Culture Collection (LEGE-CC) (https://lege.ciimar.up.pt/) (Ramos et al., 2018) was cultured and upscaled under standard conditions. A crude organic methanolic extract with a final dichloromethane extraction step was obtained from the lyophilized biomass of *Nodularia* sp. LEGE 06071 (40 g). The fractionation process was initiated by Vacuum-Liquid Chromatography. The presence of the compound on the fractions was confirmed by LC/MS analysis, and fractions with nocuolin

A were pooled together and submitted to flash chromatography with increasing polarity solvents. The chemical profile of the subsequent fractions was compared through thin-layer chromatography, and fractions were pooled according to their profile similarities. After the isolation of nocuolin A (16.4 mg) by high-pressure liquid chromatography, its abundance and purity (>99%, ^{1}H NMR) were obtained by LC-MS and ^{1}H nuclear magnetic resonance (Appendix A Fig. S1).

2.2. Antifouling bioactivity

2.2.1. Settlement inhibition bioassay using Mytilus galloprovincialis plantigrades

Small aggregates of juvenile mussels (*M. galloprovincialis*) were collected during low neap tides in intertidal pools, at Memória beach, Matosinhos, Portugal (41° 13′ 59″ N; 8° 43′ 28″ W). At the laboratory, samples were screened in a binocular magnifier (Olympus SZX2-ILLT) for mussel post-larvae - plantigrades (0.5–2 mm) (Alfaro et al., 2004; Carl et al., 2011). Mussel plantigrades displaying foot exploratory behavior were transferred to a Petri dish with filtered seawater and gently cleansed of adhered organic particles before being used in the bioassays. The settlement inhibition of *M. galloprovincialis* plantigrades bioassay followed the description in Almeida et al. (2017). Briefly, active post-larvae mussel plantigrades were exposed to nocuolin A in 24-well microplates with 4 replicates (5 plantigrades per well) for 15 h, at 18 ± 1 °C, in the darkness. Nocuolin A was screened at 12.5 and 25 μM by diluting the compound stock solution (50 mM in DMSO). Negative (0.1% DMSO) and positive controls (5 μM $CuSO_4$) were included in bioassays. All tested solutions were prepared in filtered natural seawater. After exposure, the presence/absence of efficiently attached byssal threads produced by each post-larva for all the tested conditions was used to assess the settlement inhibition.

2.2.2. Antibacterial and anti-diatom bioassays

The antibacterial activity of nocuolin A was assessed against five strains of marine biofilm-forming bacteria *Cobetia marina* CECT 4278, *Vibrio harveyi* CECT 525, *Halomonas aquamarina* CECT 5000, *Pseudoalteromonas atlantica* CECT 570, and *Roseobacter litoralis* CECT 5395 selected from the Spanish Type Culture Collection (CECT) as described in previous studies (Almeida et al., 2017; Antunes et al., 2019; Resende et al., 2021). After inoculation in Marine Broth (Condalab), bacteria were exposed to nocuolin A in 96 well flatbottom microtiter plates and incubated for 24 h (72 h for *Roseobacter litoralis*), at 26 °C. Nocuolin A was screened at 12.5 and 25 μM. Negative (1% DMSO) and positive controls (1:100 penicillin-streptomycin-neomycin stabilized solution (Sigma P4083)) were also included. Four replicates per condition were used. Initial optical density was ensured to be at 0.1 (OD600). Bacterial growth inhibition was determined at 600 nm with a microplate reader (Biotek Synergy HT, Vermont, USA).

Navicula sp. from the Spanish Collection of Algae was selected as a representative of the benthic marine diatoms, for the anti-microalgal screening, performed according to Antunes et al. (2019). Briefly, diatoms, inoculated in F/2 medium (Sigma) with silica (Sigma G9903) at an initial concentration of 2–4 x 10^4 cells mL^{-1}, were exposed to nocuolin A, at 12.5 and 25 μM, in 96 well flat-bottom microtiter plates for 10 days, at 20 °C. Negative (1% DMSO) and positive controls (3.55 μM cycloheximide) were included. Each condition was assessed in quadruplicate. Growth inhibition of diatoms was quantified by the difference in cell densities among conditions.

2.3. Antifouling mechanism of action

2.3.1. In vitro AChE inhibition assay

The *in vitro* AChE inhibition assay used Electrophorus electric AChE Type V–S (SIGMA C2888, E.C. 3.1.1.7), as described by Ellman et al. (1961) and modified by Almeida et al. (2015). The reaction solution included 30 mL of phosphate buffer (0.1 M, pH = 7.2), 1 mL of the reagent dithiobisnitrobenzoate (DTNB) at 10 nM (5,5′-Dithiobis (2-nitrobenzoic acid) and sodium hydrogen carbonate dissolved in phosphate buffer at 0.1 M, pH = 7.2) and 200 μL of acetylthiocholine iodide at 0.075 M. During the assay, 50 μL of pure AChE (0.25 U/mL) was added to 250 μL of the reaction solution, for each condition. Nocuolin A was screened at 25 and 50 μM. Negative (0.2% DMSO) and positive controls (100 μM eserine) were included. All conditions were assessed in quadruplicate. The activity of the AChE was detected at 412 nm for 5 min at 25 °C.

2.3.2. In vitro tyrosinase inhibition assay

Tyrosinase inhibition assay was conducted using *Agaricus bisporus* tyrosinase (EC 1.14.18.1) according to Adhikari et al. (2008) with appropriate adaptations (Almeida et al., 2017). Briefly, 50 μL of tyrosinase (25 U/mL) in phosphate buffer (50 mM, pH 6.5) was added to each condition. Nocuolin A was screened at 12.5 and 25 μM. The enzymatic activity was initiated by L-dopa (25 mM) also prepared in phosphate buffer (50 mM, pH 6.5). Negative (0.2% DMSO) and positive controls (100 μM kojic acid) were included. All conditions were assessed in quadruplicate. Tyrosinase activity was detected at 475 nm for 5 min at 25 °C.

2.4. Proteomic profiling of the M. galloprovincialis plantigrades

2.4.1. Sample preparation and protein extraction

M. galloprovincialis plantigrades were exposed to nocuolin A at 5 μM and 10 μM as described previously for the settlement inhibition assay. The concentration of 5 μM was selected to represent a closer concentration to the EC_{50} value observed for the mussel plantigrades while the 10 μM concentration purpose was to explore the differences in the proteomic expression of the plantigrades when exposed to higher concentrations of nocuolin A. After the exposure, mussel plantigrades from negative control (0.1% DMSO) and tested nocuolin A concentrations (5 μM and 10 μM) were collected (10 plantigrades/replicate, 3 replicates/condition). Protein extraction and subsequent proteome analysis were performed as described by Campos et al. (2016). After defrosting in ice, samples were solubilized in lysis buffer (composed of 2% (w/v) SDS, 100 mM Tris-HCl at pH 7.6, 0.1 M DTT, and 1:50 protease inhibitor) and incubated at 25 °C in the dark at 500 rpm overnight. After confirming in the stereoscope that all shells were open and empty, protein denaturation was performed for 3 min at 95 °C. The supernatant was collected, and the total protein concentration was estimated using the Bradford method, with diluted samples (1:10).

2.4.2. Filter-aided sample preparation (FASP)

Proteins were subsequently digested through filter-aided sample preparation (FASP) (Wiśniewski et al., 2009). Entire protein extracts were diluted in 200 μL of UA buffer (8 M urea, in 0.1 M Tris/HCl, pH 8.5) and transferred to filter units (Microcon 10 kDa NMWL, Merck Millipore Ltd., Tullagreen, Ireland) previously washed in water and UA buffer. After centrifugation at 14,000 G for 20 min, 100 μL of 0.05 M iodoacetamide was added to the filter units, mixed at 600 rpm in the dark, for 1 min (Thermomixer compact, Eppendorf, Hamburg, Germany), and incubated for 20 min at room temperature. Filter units were centrifuged at 14,000 G for 20 min, at room temperature, followed by two successive washings with 100 μL UA buffer, with centrifugations, and 100 μL of 0.05 M ammonium bicarbonate. Peptide digestion was initiated by adding recombinant proteomics-grade trypsin (Roche, Mannheim, Germany) at a 1:100 enzyme-to-protein ratio in 0.05 M ammonium bicarbonate to the samples. After mixing for 1 min at room temperature, samples were incubated in a wet chamber at 37 °C for 18 h. Digested peptides were eluted in new tubes by adding 50 μL of 0.5 M NaCl between centrifugations. Before desalting, the peptide concentrations were measured at 280 nm and acidified with 5 μL of formic acid (10% v/v). For peptide desalting were used C18 columns (UptiTip™ C18 Packed C18 10–200 μL, Interchim Innovations, Montluçon, France) and

conditioned with acetonitrile (60% v/v) and formic acid (0.1%, v/v), as described in the manufacturer's protocol. The samples were then added to the columns and washed with formic acid (0.1% v/v). The final elution of peptides was performed with acetonitrile (60% v/v) and formic acid (0.1%, v/v) in new tubes. The peptide concentration was measured at a wavelength of 280 nm. The samples were dried in a vacuum concentrator (Concentrator Plus ™, Eppendorf).

2.4.3. LC-MS analysis

Obtained peptides were analyzed by nano-LC coupled to a hybrid Ion trap-Orbitrap mass spectrometer (LTQ Orbitrap Velos Pro, Thermo Scientific, Waltham, EUA). Full scans were performed at 30,000 resolution with scan ranges of 380–2000 *m/z* and the top 20 most intense ions isolated and fragmented. Collision-induced fragmentation (CID) was used to fragment precursor ions. Charge state deconvolution and deisotoping were not performed. All MS/MS spectra were analyzed using Sequest (Thermo Fisher Scientific, San Jose, CA, USA; version IseNode in Proteome Discoverer 2.4.0.305). Sequest was set up to search Mollusca 20201001.fasta (unknown version, 365732 entries, UniProtKB database) assuming the digestion enzyme trypsin. Sequest was searched with a fragment ion mass tolerance of 0.020 Da and a parent ion tolerance of 10.0 PPM. Carbamidomethyl of cysteine was specified in Sequest as a fixed modification. Oxidation of methionine was specified in Sequest as a variable modification.

2.4.4. Protein identification and quantification

Scaffold program (version Scaffold_4.11.1, Proteome Software Inc., Portland, OR) was used to validate MS/MS-based peptide and protein identification. Peptide identifications were accepted if they could be established at greater than 95.0% probability by the Percolator posterior error probability calculation (Käll et al., 2008). Protein identification was accepted if they could be established at greater than 99.0% probability and contained at least two identified peptides. Protein probabilities were assigned using the Protein Prophet algorithm (Nesvizhskii et al., 2003). Proteins that contained similar peptides and could not be differentiated by MS/MS analysis alone were grouped to satisfy the principles of parsimony. Proteins that shared significant peptide evidence were grouped into clusters.

2.4.5. Functional classification of protein and pathways analysis

Obtained protein sequences were compared (blast) against *the Crassostrea gigas* sequences (91.786 sequences, downloaded from UniProt Knowledgebase release 2023_05 (Bateman et al., 2023), and cgigas_uk_roslin_v1 peptide sequences 2023_11, downloaded from Ensembl Metazoa), using the local BLASTp function from Blast2GO version 6.0.3 (basic) (Conesa et al., 2005; Conesa and Götz, 2008; Götz et al., 2008), with a cut-off e-value of 1 x 10^{-3}. This analysis was required due to the insufficient annotation of the *M. galloprovincialis* protein sequence. A multi-query analysis compared homologous *C. gigas* sequences from both concentrations, grouping them into functional classes (Gene Ontology classes) through the g:OSt function in g:Profiler (version e111_eg58_p18_30541362). Statistically significant enriched biological processes, molecular functions, and cellular components were detected using a hypergeometric test. Results were validated with Benjamini--Hochberg's false discovery rate correction (p-value <0.05) (Kolberg et al., 2023). A functional network was constructed on Cytoscape version 3.10.2 (Shannon et al., 2003).

2.5. Ecotoxicity assessment

2.5.1. Artemia salina bioassay

The brine shrimp (*A. salina*) nauplii lethality test was used to assess the general marine ecotoxicity of the nocuolin A (Almeida et al., 2017). Nauplii hatched in nutrient-enriched seawater after approximately 24 h at 26 °C. Initially, nocuolin A concentrations of 12.5 and 25 μM were evaluated. The lethality tests were performed with 15–20 nauplii per well, eight replicates per condition, in 96-well microplates in darkness, at 25 °C, for 48 h. A negative (1% DMSO) and a positive control (13.6 μM $K_2Cr_2O_7$) were included in the assays.

2.5.2. Amphibalanus amphitrite bioassay

The barnacle *Amphibalanus amphitrite* was used to perform a nauplii lethality test (Piazza et al., 2012; Rittschof et al., 1992). Adult barnacle broods were brought from the field, cleaned from epibionts, and maintained in the lab, in filtered natural seawater (FNSW) at room temperature (22 ± 5 °C). The broodstock was fed a mixture of microalgae (*T-iso lutea*, *Tetraselmis suecica,* and *Dunaliella tertiolecta*, every day) and newly hatched brine shrimp (*A. salina* every other day) *ad libitum*. Whenever nauplii are needed, adult barnacles are left dried overnight and, the next morning, FNSW at 28 °C was added to the beaker and placed in the dark near a pointed light source to stimulate the release of the nauplii. Nauplii were collected using a Pasteur pipette and transferred to another beaker with FNSW to release them from debris and ensure they were actively swimming. Toxicity tests were conducted in glass tubes containing 3 mL of test solutions (3 replicates) using newly hatched nauplii collected less than 3 h after release from adult barnacles. The assay consisted of adding a drop of these larvae (50 μL, 30−60 larvae) to each test tube and incubating at 28 °C in darkness without feeding for 24 h. Mortality was determined as the proportion of immotile nauplii. Controls and solvent controls (0.1% DMSO) were included in the assays which were repeated twice. Data was combined for statistical analysis.

2.5.3. Zebrafish embryo Acute toxicity test (ZFET)

Zebrafish (*Danio rerio*) embryos were used to assess the lethal and sub-lethal effects of nocuolin A. Breeding maintenance and embryo collection was conducted in our certified Bioterium of Aquatic Organisms (BOGA, CIIMAR, Porto). All experiments were conducted following ethical guidelines of the European Union Council (Directive, 2010/63/EU) and the Portuguese Ministry of Agriculture, Sea, Environment, and Spatial Planning (Decree-Law nr. 113/2013, 7 August) for the protection of animals used for experimental and other scientific purposes.

Fish embryo exposures were conducted in an E3 medium (pH 8.6) following an adaptation of the OECD guideline (OECD, 2013) using 96-well plates. Briefly, newly fertilized eggs were exposed to a range of nocuolin A concentrations (ten embryos per concentration) from approximately 1 h post-fertilization (hpf) until 96 hpf at 28 °C. Embryos were inspected under a microscope every 24 h for lethal and sub-lethal effects, with solution renewal at each inspection. Indicators of lethality included coagulation of fertilized eggs, absence of heartbeat or somite formation, and failure of tail detachment from the yolk sac. Recorded sub-lethal endpoints included hatching time, tail deformities, presence of heart or yolk sac edema, and locomotion difficulties. Controls and solvent controls (DMSO 0.1%) were included in the assays. The assay was repeated three times.

2.5.4. In silico predictions of nocuolin A

Based on the molecular structure of a given substance, it is possible to predict important parameters related to its physicochemical properties and PBT (persistence, bioaccumulation, and toxicity) criteria. This is particularly relevant when little or no information exists. In this study, we used EPISUITE™, a Windows-based suite of programs developed by the U.S. Environmental Protection Agency (EPA's Office of Pollution Prevention Toxics) and Syracuse Research Corporation (SRC), to estimate the physicochemical properties and environmental fate of nocuolin A. Input values included the compound name, molecular weight, chemical formula, and SMILES notation. To distinguish nocuolin A between a baseline toxicant or a specifically toxic substance, we used the Toxic Ratio, which is the ratio between an estimated LC_{50} (using a QSAR - quantitative structure-activity relationship - a model for baseline toxicity) and the experimental LC_{50} value for the given species (Maeder et al., 2004). To assess the potential ecological risk of nocuolin A, we used MAMPEC (Marine Antifoulant Model to Predict Environmental

Concentrations, Version 3.0; Deltares, Netherlands) to calculate the predicted environmental concentrations (PEC). MAMPEC can predict environmental concentrations by considering different environments (e.g., harbors, marinas), emission scenarios (including leaching rates, underwater surface area, and shipping characteristics), and the antifoulant's physicochemical properties (Van Hattum et al., 2006). For input values, we followed the approach established by the OECD-EU working group for the risk assessment of antifoulants in an OECD commercial harbor environment and emission scenario descriptors (OECD, 2004) without modifications. The compound descriptor input values included the molecular formula and mass, and values estimated with EPISUITE™ (US EPA, 2016), such as solubility, octanol-water partition coefficient (Log K_{OW}), and partition coefficient (Log K_{OC}).

2.6. Data analysis

All data were first checked for normality (Kolmogorov–Smirnov test) and homogeneity of variances (Levene's test), and appropriate transformations were made when necessary. Data from the nocuolin A screening activities across all bioassays were analyzed using one-way analysis of variance (ANOVA) followed by Dunnett's test ($p < 0.01$). ANOVA analysis was also applied to determine the values for no observed effect concentration (NOEC) and lowest observed effect concentration (LOEC) in the ecotoxicity assessment assays. The half-maximal effective concentrations (EC_{50}) were determined for the settlement inhibition of *M. galloprovincialis* plantigrades and the growth inhibition of *Navicula* sp. The median lethal dose (LC_{50}) was also assessed for those assays and also for the *A. salina* nauplii, *A. amphitrite* nauplii, and *D. rerio* embryo toxicity assays. Probit regression analysis was employed to calculate EC_{50} and LC_{50} values. The Pearson Goodness-of-Fit Chi-Square test ($p < 0.01$) was applied to the Probit regression analysis, with 95% lower and upper confidence limits (95% LCL; UCL). ANOVA and Probit analyses were conducted using IBM SPSS Statistics 28. The therapeutic ratio (LC_{50}/EC_{50}) was used to evaluate the compound's effectiveness versus toxicity (Almeida et al., 2017; Qian et al., 2010b; Rittschof et al., 2003). For proteomic data, differentially expressed proteins (DEPs) were assessed using the "DEP" R package, with R: a language and environment for statistical computing version 4.3.3 (R Core Team, 2021; Zhang et al., 2018). Significant differences between nocuolin A and control conditions were identified by applying a $\log_2$ fold change (lfc = $\log_2(1.5)$) as a threshold to classify proteins as DEPs.

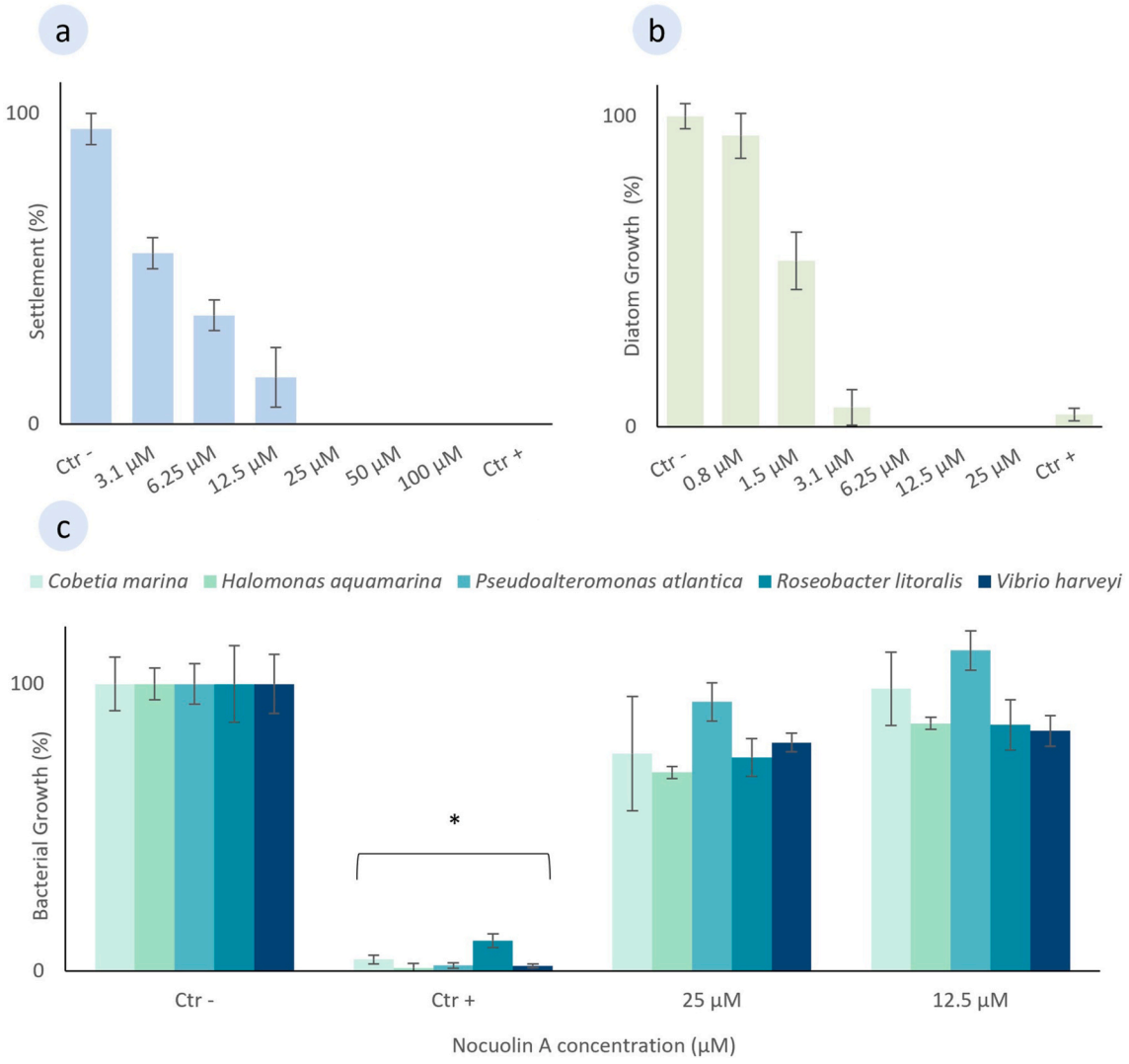

Fig. 2. Antifouling activity of nocuolin A against target organisms. (a) Dose-response curve of the settlement inhibition activity in M. galloprovincialis plantigrades. Ctr-: DMSO (0.1%), Ctr+: $CuSO_4$ (5 µM); (b) Dose-response curve of the growth inhibition of Navicula sp. Ctr-: DMSO (1%), Ctr+: Cycloheximide (3.55 µM); (c) Growth inhibition of five marine biofilm-forming bacteria screening bioassay, where the compound was tested at 12.5 and 25 µM. Ctr-: DMSO (1%), Ctr+: 1:100 penicillin-streptomycin-neomycin stabilized solution. *Significant differences compared to the negative control ($p < 0.01$, Dunnett's test).

3. Results

3.1. Antifouling activity of nocuolin A

The AF activity of nocuolin A was characterized using both micro and macroorganisms representative of marine biofouling communities. *M. galloprovincialis* was selected for the settlement inhibition assay due to its prominence as a marine macrofouling organism and model species in AF bioassays (Neves et al., 2022). Screening of nocuolin A at 12.5 and 25 μM against mussel post-larvae (plantigrades) was performed to assess their ability to resettle (anti-settlement activity). Significant settlement inhibition ($p < 0.01$) was observed at both concentrations (15 ± 9.6% and 0 ± 0% of settlement, respectively). Further bioassays were performed to determine the half-maximal effective concentration (EC_{50}) that inhibited 50% of the mussel plantigrades settlement, which was found to be 3.905 μM (Fig. 2 a). For the assessment of microfouling organisms, five marine biofilm-forming marine bacteria and microalgae (the diatom *Navicula* sp.) were used for growth inhibition assays. Diatoms were exposed to nocuolin A for 10 days in an initial screening at 12.5 and 25 μM, resulting in high mortality (100 ± 0%) at these concentrations. Lower concentrations were tested (25, 12.5, 6.2, 3.1, 1.5, and 0.8 μM) and an EC_{50} value of 1.561 μM was determined in the dose-response assay for nocuolin A (Fig. 2 b). In addition, five marine biofilm-forming bacterial strains (*Cobetia marina*, *Vibrio harveyi*, *Halomonas aquamarina*, *Pseudoalteromonas atlantica*, and *Roseobacter litoralis*) were exposed to nocuolin A, at 12.5 and 25 μM, for 24 h, except for *R. litoralis*, which was exposed for 72 h. Promising antibacterial activity was considered if a threshold of ≥30% of growth inhibition was achieved. However, nocuolin A showed no significant inhibition of bacterial growth for any of the tested marine bacterial strains (Fig. 2 c).

3.2. In vitro enzymatic inhibition assays for AChE and tyrosinase

AChE and tyrosinase assays were conducted to evaluate a possible molecular target that could be implicated in the AF activity of nocuolin A, as these pathways are involved in mussel adhesion mechanisms. The enzymatic assays revealed no inhibition of AChE or tyrosinase activities compared to the negative control, excluding these pathways as possible molecular targets for nocuolin A (Fig. 3).

3.3. Proteomic profiling of the M. galloprovincialis plantigrades

The putative effect of nocuolin A on mussel plantigrades at a molecular level was further investigated by shotgun proteomic analysis. Plantigrades were exposed to two concentrations of nocuolin A (5 and 10 μM) and compared to a control group (0.1% DMSO). The analysis identified 1718 proteins. Since a low number of proteins was identified in one of the three replicates representing the 5 μM nocuolin A group, this sample was excluded, and the analysis continued with only two replicates for this concentration. Therefore, changes in protein expression were analyzed using fold change (log_2 fold change of 1.5). In total, 222 proteins were differentially expressed across all conditions (Appendix A Supplementary Table S1). Fig. 4 a presents the proteomic profile in a heatmap, where rows represent the differentially expressed proteins and their relative expression levels under different conditions (control, 5 μM nocuolin A, and 10 μM nocuolin A). Proteins were clustered with distances between clusters indicating differences in expression levels. The heatmap columns correspond to the three experimental conditions. The color gradient in the heatmap shows variations in protein expression across different conditions. The Venn diagram in Fig. 4 b shows that out of the 222 DEPs, 18 were common to nocuolin A groups when compared to the control. In contrast, 61 and 48 DEPs were unique to the 5 μM and 10 μM groups, respectively. Notably, the presence of precollagen NG (Q8MW55) and precollagen D (O44367) among the identified proteins was observed, as these are constituents of the mussel byssal threads. However, none of these proteins were classified as differentially expressed when comparing the nocuolin A conditions with the negative control after applying the log_2 fold change of 1.5 threshold.

Further insights into the molecular processes of the differentially expressed proteins affected by nocuolin A were investigated through functional enrichment analysis. Homologous *Crassostrea gigas* sequences (phylogenetically closer species available) were classified using gene ontology (GO) terminology and grouped according to their functions. Blast results are displayed in Appendix A Supplementary Table S2. Functional classes were searched using the web tool g:Profiler, and statistically significant enriched biological processes, molecular functions, and cellular components were filtered using a hypergeometric test (Fisher's exact test, p-value <0.05) with Benjamini-Hochberg's false discovery rate correction. The resulting functional network is illustrated in Fig. 5. This analysis retrieved 49 GO terms describing the functions of differentially expressed proteins (Appendix A Supplementary Table S3). Most GO terms belonged to the cellular components category and were identified for both concentrations. Clusters in cellular components, common to both concentrations, included protein and ribonucleoprotein complexes (AP-2 complex subunit alpha (K1QAB1), eukaryotic translation initiation factor 3 subunit A (A0A8W8INP3), eukaryotic translation initiation factor 3 subunit B (A0A8W8HZ31), RRM domain-containing protein (A0A8W8IE27), Arp2/3 complex 34 kDa subunit

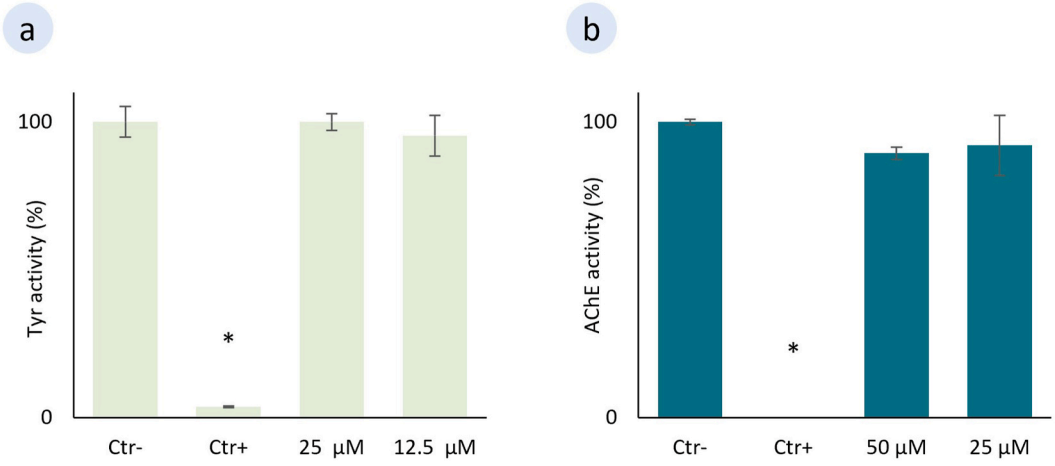

Fig. 3. In vitro enzymatic inhibition assays of nocuolin A. (a) Tyrosinase inhibition. Ctr-: DMSO (0.2%); Ctr+: Kojic acid (100 μM). (b) AChE inhibition. Ctr-: DMSO (0.2%); Ctr+: Eserine (100 μM).*Significant differences compared to the negative control ($p < 0.01$, Dunnett's test).

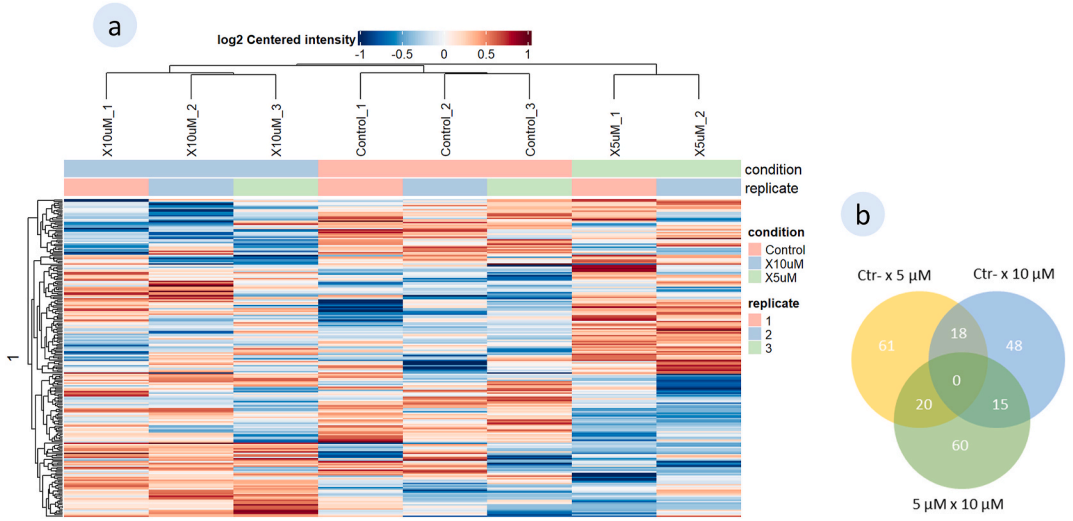

Fig. 4. Heatmap and Venn's diagram showing differently expressed proteins (DEPs) in mussel plantigrades when exposed to nocuolin A at 5 and 10 µM and control. (a) The heatmap illustrates DEPs for each condition, showing the differences as a $\log_2$ fold change of 1.5, depicted in a color map (red: upregulated; blue: down-regulated). The rows represent DEPs clustered by k-means clustering (1). The columns represent the tested conditions: DMSO 0.1% (control), nocuolin A concentrations at 5 µM (x5uM), and 10 µM (x10uM). (b) The Venn diagram highlights the number of unique and shared DEPs identified by pairwise comparisons between each condition. (For interpretation of the references to color in this figure legend, the reader is referred to the Web version of this article.)

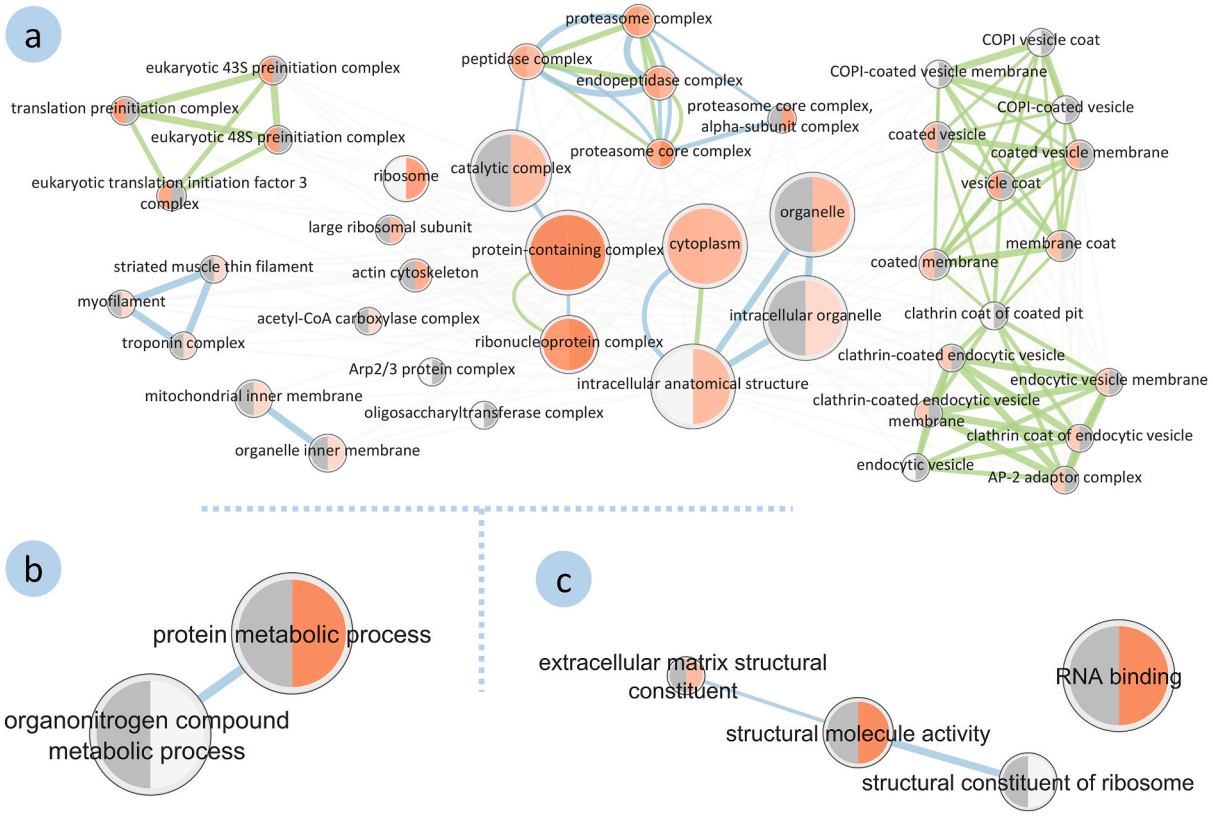

Fig. 5. Functional network of differentially expressed proteins in the mussel plantigrades exposed to nocuolin A at 5 and 10 µM. The GO categories represented include (a) Cellular Components, (b) Biological Processes, and (c) Molecular Functions. Node sizes increase with the number of proteins associated with that GO term and color intensifies with significance (FDR q-value cut-off = 0.05; p-value cut-off = 0.05; grey means the absence of proteins for the GO term. Nodes are divided, representing the different tested concentrations of nocuolin A, at 5 (left side) and 10 µM (right side). Green edges link functions identified in samples exposed to 5 µM while blue edges connect functions from samples exposed to 10 µM. (For interpretation of the references to color in this figure legend, the reader is referred to the Web version of this article.)

(A0A8W8M9C6), 26S proteasome non-ATPase regulatory subunit 6 (K1QUE6), proteasome subunit beta (A0A8W8KC84), collagen alpha-2 (I) chain (K1PDS7), dolichyl-diphosphooligosaccharide-protein glycosyltransferase subunit 2 (K1QHM2), proteasome subunit alpha type (A0A8W8JYP9), 40S ribosomal protein S25 (A0A8W8LCY1), 60S ribosomal protein L21 (A0A8W8L8N9), large ribosomal subunit protein

eL30 (A0A8W8NG46), 60S ribosomal protein L13 (A0A8W8JYD4), cyclic nucleotide-binding domain-containing protein (A0A8W8MFI8), 60 kDa SS-A/Ro ribonucleoprotein (K1QRQ0), KOW domain-containing protein (A0A8W8IPA8), splicing factor 3B subunit 1 domain-containing protein (A0A8W8M508), collagen alpha-2(I) chain (A0A8W8NCS6), fibrillar collagen NC1 domain-containing protein (A0A8W8KPZ6), myosin-XV (K1RD93), proteasome subunit alpha type (A0A8W8J5Q6), proteasome subunit beta (K1QBT2), protein transport protein SEC23 (A0A8W8IF30), and succinate dehydrogenase (A0A8W8N2K5)); and peptidase/proteasome complex (26S proteasome non-ATPase regulatory subunit 6 (K1QUE6), proteasome subunit alpha type (A0A8W8JYP9), proteasome subunit beta (K1QBT2)). Regarding the clusters from cellular components only present for 5 μM of nocuolin A, these include the vesicle components group (coatomer subunit delta (A0A8W8KS23), and AP-2 complex subunit alpha (K1QAB1) and the eukaryotic translation complex (eukaryotic translation initiation factor 3 subunit A (A0A8W8INP3), eukaryotic translation initiation factor 3 subunit B (A0A8W8HZ31)). In contrast, the cellular components exclusively found at 10 μM nocuolin A, were related to the muscle constituent group, which included striated muscle thin filament, troponin complex, and myofilament, which all shared the association to the same protein, troponin T (A0A8W8NMI9), the mitochondrial membrane group (cytochrome *c* oxidase subunit 5A, mitochondrial (K1PVD7), calcium-binding mitochondrial carrier protein SCaMC-2 (K1QR48), succinate dehydrogenase (A0A8W8N2K5)), the actin cytoskeleton (Arp2/3 complex 34 kDa subunit (A0A8W8M9C6), myosin-XV (K1RD93), and troponin T (A0A8W8NMI9)) and ribosome constituents (60S ribosomal protein L13 (A0A8W8JYD4), KOW domain-containing protein (A0A8W8IPA8), 40S ribosomal protein S25 (A0A8W8LCY1), large ribosomal subunit protein uL1 (A0A8W8MU73), and 60S ribosomal protein L21 (A0A8W8L8N9)). For other functional categories, such as molecular functions and biological processes, the GO terms were only found for the 10 μM concentration. Clusters related to biological processes included protein metabolism and organonitrogen compounds (calpain-5 (K1R1C6), 60S ribosomal protein L13 (A0A8W8JYD4), calcium/calmodulin-dependent protein kinase (A0A8W8ID93), cyclic nucleotide-binding domain-containing protein (A0A8W8MFI8), inter-alpha-trypsin inhibitor heavy chain H3 (A0A8W8LTT6), KOW domain-containing protein (A0A8W8IPA8), mitogen-activated protein kinase (A0A8W8KPG9), transmembrane 9 superfamily member (A0A8W8MZX0), dolichyl-diphosphooligosaccharide-protein glycosyltransferase subunit 2 (K1QHM2), transglutaminase-like domain-containing protein (A0A8W8JUK3), counting factor associated protein D (A0A8W8NWQ5), proteasome subunit alpha type (A0A8W8J5Q6), proteasome subunit alpha type (A0A8W8JYP9), proteasome subunit beta (K1QBT2), laminin G domain-containing protein (A0A8W8LGH4), ubiquitin carboxyl-terminal hydrolase (K1PX47), heat shock 70 kDa protein 12B (A0A8W8L019), large ribosomal subunit protein uL1 (A0A8W8MU73), argininosuccinate lyase (A0A8W8JQ38), and 60S ribosomal protein L21 (A0A8W8L8N9)). Clusters identified in molecular functions were related to RNA binding, structural molecular activity, extracellular matrix structural constituent, and structural constituent of ribosome, sharing most of the associated proteins (60S ribosomal protein L13 (A0A8W8JYD4), KOW domain-containing protein (A0A8W8IPA8), collagen alpha-2(I) chain (A0A8W8NCS6), fibrillar collagen NC1 domain-containing protein (A0A8W8KPZ6), large ribosomal subunit protein uL1 (A0A8W8MU73), methenyltetrahydrofolate synthetase domain-containing protein (K1QRL6) and 60S ribosomal protein L21 (A0A8W8L8N9)). The overall response of the mussel plantigrades to nocuolin A was characterized by a general stress response, followed by muscle dysregulation, impairment of energy production, and endoplasmic reticulum stress.

3.4. Ecotoxicity assessment

3.4.1. In vivo effects of nocuolin A

In parallel with the AF activity assessment, the toxicity of nocuolin A on target biofouling organisms was also evaluated (Table 1). No lethal effects were observed on the mussel plantigrades exposed to the compound at any of the tested concentrations. The non-toxic impact on the mussel plantigrades was based on the $LC_{50} > 100$ μM (>29.843 μg mL^{-1}) and a therapeutic ratio higher than 15 ($LC_{50}/EC_{50} = 25.61$). Toxicity was also assessed on the macrofouling species *A. amphitrite*, being the nauplii larval stage used for the toxicity tests (Piazza et al., 2012; Rittschof et al., 1992). The compound exhibited a significantly lower LC_{50} (0.016 μM; 0.00483 μg mL^{-1}) for barnacle larvae when compared to the mussel plantigrades, indicating higher toxicity to the early stages of barnacle development. The NOEC and LOEC values for barnacle larvae were 0.001 μg mL^{-1} and 0.239 μg mL^{-1}.

For marine biofilm-forming bacterial strains, no toxic effects were observed as there was no growth inhibition after exposure to nocuolin A (Fig. 2 c). However, high mortality was noted in the exposed diatom cells for the screened concentrations (12.5 and 25 μM, 3.730 and 7.461 μg mL^{-1}, respectively) with an $LC_{50} > 3.1$ μM (>0.925 μg mL^{-1}). The toxicity of nocuolin A towards *Navicula* sp. was further confirmed by the lower therapeutic ratio ($LC_{50}/EC_{50} = 1.986$).

Beyond considering the target organisms, two more species (*A. salina* and *D. rerio*) were selected to evaluate the environmental toxicity of nocuolin A. All bioassays met the requirements for control survival and normal development (≥90%). No significant differences were observed between the control and solvent control groups; thus, treatments were compared to the respective DMSO control (0.1%). Nominal concentrations were used throughout this study. LC_{50} values are summarized in Table 2.

The crustacean *A. salina* nauplii, a model species widely used in ecotoxicology, exhibited an LC_{50} value of 2.480 μM (0.740 μg mL^{-1}), with NOEC and LOEC values of 0.0025 μg mL^{-1} and 0.448 μg mL^{-1}, respectively. In comparison to the LC_{50} values of *A. salina* and *A. amphitrite* nauplii, the barnacle nauplii displayed higher sensitivity to the compound, with LC_{50} values lower by two orders of magnitude. The zebrafish assay revealed a 96h-LC_{50} of 0.0584 μM; 0.0174 μg mL^{-1}, with almost no sublethal effects detected.

3.4.2. In silico predictions of nocuolin A

The predicted data obtained from the EPI Suite™ for nocuolin A is shown in Table 2 and 3. In ecotoxicology, the octanol/water partition coefficient (also known as log K_{ow} or Log P) indicates the bioconcentration potential of a substance. It has been demonstrated that a log $K_{ow} > 4.5$ may pose a risk for marine organisms since suggests a high affinity for lipids in an organism (Gimeno et al., 2024). Nocuolin A's log K_{ow} is precisely at this threshold. Nevertheless, the BCF value obtained for nocuolin A is much lower than 2000 L Kg^{-1}, which is the threshold used to classify a bioaccumulative substance. The BCF value is the result of a balance between the rate of chemical uptake from water and its elimination from the organism, indicating a reduced bioconcentration potential in marine organisms. BCF should not be used alone to model bioaccumulation of contaminants; however, it is very useful, especially for initial screening (Wang, 2016).

In addition, we used ECOSAR, which is a computerized predictive system that estimates aquatic toxicity, to obtain LC_{50}s calculated using a QSAR (quantitative structure-activity relationship) model for baseline toxicity, for several model organisms. By comparing the estimated LC_{50} with the experimental value, for the same species, one can obtain a Toxic Ratio (TR). This ratio can be used to distinguish "specifically toxic chemicals" from "baseline toxicants" considering a threshold of TR = 10 (Maeder et al., 2004). In this study, we used zebrafish for these calculations and obtained a TR of 20.4 or 79.5 depending on if nocuolin A is considered more similar to a hydrazine or an amide, respectively. The threshold of 10 was surpassed, although not by much, meaning that this

Table 1
Antifouling effectiveness versus toxicity of nocuolin A towards biofouling organisms. The half maximum effective concentration (EC_{50}), the median lethal concentration (LC_{50}), no observed effect concentration (NOEC), lowest observed effect concentration (LOEC), and the therapeutic ratio (LC_{50}/EC_{50}) are listed. The EC_{50}, LC_{50}, NOEC, and LOEC are provided in both μM and μg mL^{-1} for comparative purposes. Confidence intervals for EC_{50} values are presented in μM (in parentheses). n.a. – not assessed.

Target species	EC_{50} (μM; μg mL^{-1})	LC_{50} (μM; μg mL^{-1})	NOEC (μM; μg mL^{-1})	LOEC (μM; μg mL^{-1})	LC_{50}/EC_{50}
M. galloprovincialis	3.905 (95 % CI: 2.866–4.860); 1.165	>100; >29.843	n.a.	n.a.	25.61
A. amphitrite	n.a.	0.0162 (95 % CI: 0.0138–0.0187); 0.00483	0.00335; 0.001	0.00838; 0.0025	n.a.
Navicula sp.	1.561 (95 % CI: 1.460–1.671); 0.466	>3.1; >0.925	n.a.	n.a.	1.986

Table 2
Toxicity of nocuolin A towards marine and freshwater organisms. The median lethal concentration (LC_{50}), no observed effect concentration (NOEC) and lowest observed effect concentration (LOEC) are presented in both μM and μg mL^{-1} for comparative purposes. Confidence intervals are displayed in μM, in parenthesis, for the LC_{50} values. n.a. – not assessed.

Species	LC_{50} (μM; μg mL^{-1})	NOEC (μM; μg mL^{-1})	LOEC (μM; μg mL^{-1})
Artemia salina	2.480 (95% CI: 2.321–2.648); 0.740	0.8; 0.239	1.5; 0.448
Danio rerio	0.0584 (95% CI: 0.0462–0.0768); 0.0174	0.0503; 0.015	n.a.

compound may reveal a specific mode of toxic action.

To perform a quantitative risk characterization, we employed an established approach by calculating the ratio between the predicted environmental concentration (PEC; calculated with MAMPEC) and the predicted no-effect concentrations (PNEC; derived from toxicity data). If this ratio is > 1, then the compound has the potential to threaten wildlife and ecosystems (European Commission, 2003). Assuming that nocuolin A would be used as an AF biocide in marine coatings, the marine antifoulant model MAMPEC was used to predict the maximum and minimum theoretical environmental concentrations (PEC_{MAX} and PEC_{MIN}). Values varied between a PEC_{MAX} of 8.56 x 10^{-5} μg mL^{-1} and a PEC_{MIN} of 5.55 x 10^{-6} μg mL^{-1} (Table 4). For PNEC calculations, all available toxicity data can be used. Regardless, the use of safety factors is strongly recommended to ensure that the potential for adverse effects on the environment is identified (European Commission, 2003). It should be noted that the safety factors to be applied are strongly associated with the type of toxicity data available. Guidance on this issue is provided in the Technical Guidance Document on Risk Assessment, in support of several directives relating to the risk assessment of new and/or existing substances and relating to the placing of biocidal products on the market (European Commission, 2003). According to this document, the PNEC was thus derived from the lowest LC_{50} or EC_{50} of the most sensitive species, on which a safety factor of 1000 times was applied. The guidelines suggest higher safety values whenever there is scarce information on toxicity (short-term LC_{50} of freshwater or saltwater representatives of three taxonomic groups). However, we consider that if this information is based on highly sensitive tests using early life stages of organisms including 3 trophic levels (algae, crustacean, and fish) plus toxicity to larvae of other marine species, the choice of a safety factor of 1000 seems more appropriate.

4. Discussion

This is the first report considering nocuolin A as a potential AF agent. In this work, nocuolin A's AF activity was assessed against a panel of microfouling species (five strains of marine biofilm-forming bacteria and a strain of a marine biofilm-forming diatom) as well as a widely occurring macrofouling species. Despite the inherent challenge of developing a leading AF agent effective across diverse biological targets acting against different fouling species, it is widely assumed that broad-spectrum and non-toxic AF agents are difficult to achieve. To ensure efficacy, mixtures of narrow-spectrum bioactive components might be applied in new AF technologies (Cahill et al., 2024). The prevention of marine bacteria and diatoms growth and, therefore, the formation of biofilms can interfere with further colonization of submerged surfaces by marine invertebrate larvae and macroalgal spores, since natural marine biofilms can modulate the colonization cascade of biofouling communities (Qian et al., 2022; Vinagre et al., 2020). Nocuolin A exhibited different effects on the growth of marine biofilm-forming bacteria and diatoms. No significant growth inhibition was found for any of the five tested marine bacterial strains. However, the compound proved to be active against the diatom *Navicula* sp. Xu and colleagues (Xu et al., 2019) also found active natural compounds against diatoms, namely cochliomysin G, a resorcyclic acid lactone isolated from the culture broth of the marine-derived fungus *Cochliobolus lunatusthe* (EC_{50} = 0.61 μg mL^{-1} for *Navicula exigua*), and zeaenol, its analogue (EC_{50} values of 3.20 and 8.71 μg mL^{-1}, for *Navicula levissima* and *Navicula exigua,* respectively). After comparing the EC_{50} values of these compounds with the one obtained for nocuolin A (EC_{50} = 0.466 μg mL^{-1}), our compound exerted a more potent activity towards the diatom. Approved AF compounds that are reported to exert antialgal toxicity (Irgarol 1051, Dichlofluanid, Tolyfluanid, Chlorothalonil, Sea-Nine 211) are described as acting as photosynthesis and carbon incorporation inhibitors and/or cell membrane disruptors through apoptosis (Chen and Qian, 2017). Regarding antibacterial activity, the most reported specific targets are related with quorum sensing inhibition (N-acyl homoserine lactone autoinducers) (Chen and Qian, 2017). A specific mode of action associated with microalgae (e.g. photosynthesis-related) could explain the differential response observed between bacteria and microalgae in

Table 4
Putative Risk Assessment based on the maximum and minimum MAMPEC-predicted environmental concentrations (PEC_{MAX} and PEC_{MIN}, (in μg mL^{-1}) in a marine commercial harbour, divided by the PNEC to which an assessment factor of 1000 was applied.

Compound	Endpoint used for PNEC estimation (μg mL^{-1})	PEC Commercial harbour (μg mL^{-1})		Risk Assessment	
		MAX	MIN	PEC_{MAX}/PNEC	PEC_{MIN}/PNEC
Nocuolin A	0.00483	8.56 x 10^{-5}	5.55 x 10^{-6}	17.72	1.15

Table 3
Predicted data from EPI Suite™ regarding biodegradability, sediment-water partition (Log K_{oc}), octanol-water partition (Log K_{ow}), and bioconcentration factor (BCF) of nocuolin A. [1]DNBF: Does Not Biodegrade Fast.

BIOWIN™			KOCWIN™	KOWWIN™	BCFBAF™
Ultimate biodegradation Days-Weeks (3.2963)	Aerobic conditions Days (4.0848)	Anaerobic conditions DNBF[1] (0.3536)	Log K_{oc} 3.0155	Log K_{ow} 4.53	BCF (LKg/wet-wt) 19.1 (1.28)

this study. In addition, from a chemical ecology perspective, the demonstrated AF activity profile of nocuolin A against microalgae may offer insights into its natural ecological function in cyanobacteria, likely conferring allelopathic properties to the host strains against competing eukaryotic microbial communities (Leão et al., 2009; Scholz and Liebezeit, 2012).

Alongside the microfouling screening, nocuolin A's activity was also assessed against plantigrades of the macrofouling species *M. galloprovincialis*. In addition to being among the most prominent macrofouling organisms worldwide, it is considered a model macrofouling species for settlement inhibition bioassays (Almeida et al., 2015, 2017, 2018; Antunes et al., 2019; Mabrouk et al., 2020; Vilas-Boas et al., 2020, 2021). Regarding the anti-settlement activity, nocuolin A exhibited an EC_{50} of 1.165 μg mL^{-1} which is considerably lower than the reference threshold (EC_{50} < 25 μg mL^{-1}) defined by the U.S. Navy program. When comparing the activity against macrofouling organisms (*Amphibalanus amphitrite* cyprids) of natural compounds isolated from cyanobacteria, nocuolin A could be ranked among the most potent cyanobacterial compounds, such as lyngbyabellins O and P (EC_{50} = 0.24–0.62 μg mL^{-1}, respectively) isolated from *Okeania* sp. (Petitbois et al., 2017) and majusculamide A and dolastatin 16 (EC_{50} = 0.54–0.003 μg mL^{-1}, respectively) isolated from *Lyngbya majuscula* (Tan et al., 2010). Compared with phidianidine A, a natural compound exhibiting a 1,2,4-oxadiazole ring linked to the brominated indole system that prevented the settlement of *Amphibalanus improvisus* cyprids at 4.0 μg mL^{-1} (Labriere et al., 2020), nocuolin A was also found to be a more potent AF compound. It is important to note that the model macrofouling species used in those bioassays was *Amphibalanus amphitrite* cyprids, rather than the *M. galloprovincialis* plantigrades used in this study, which implies different sensitivities, as mussel plantigrades are usually more robust. When directly compared with a compound derived from cyanobacteria tested on the same target organism, such as portoamides (EC_{50} = 4.86 μg mL^{-1}), cyclic peptides isolated from *Phormidium* sp. LEGE 05292 in our group (Antunes et al., 2019), nocuolin A demonstrated significantly stronger activity. Nocuolin A's activity against *M. galloprovincialis* plantigrades is also comparable in potency to other natural compounds isolated from marine actinomycetes *Streptomyces aculeolatus*, namely napyradiomycins (EC_{50} = 0.1–6.34 μg mL^{-1}), madeirone and neomadeirone (EC_{50} = 1.76 and 0.12 μg mL^{-1}, respectively) (Pereira et al., 2020; Wissner et al., 2024). A similar conclusion can be drawn by comparing the activity of the commercial AF agent ECONEA® (EC_{50} = 1.40 μg mL^{-1}) on mussel plantigrades (Almeida et al., 2017).

As previously discussed, the distinctive effect of nocuolin A on the tested bacteria (non-active) compared to diatom species and mussel plantigrades (active) suggests that the underlying mechanistic action and biological targets of nocuolin A may involve different eukaryotic pathways. A similar multi-action behavior has been reported for alkyl triphenylphosphonium salts, which act as non-toxic quorum sensing disruptors in marine bacteria and tyrosinase inhibitors for byssal production in the mussel *M. galloprovincialis* (Martín-Rodríguez et al., 2015), as well as for the AF compounds 7-Hydroxy-4-methylcoumarin (Pérez et al., 2016), the bromotyrosine derivative ianthelline (Hanssen et al., 2014), 3-Alkylpyridinium oligomers and polymers (3-APS) (Grandič et al., 2012), among others. Given this complexity, elucidating the mechanisms of action for AF compounds has become essential for the development of new AF agents (Chen and Qian, 2017), though a single molecular target or pathway may not always be identifiable due to the intricate biological processes involved in biofouling colonization (Cahill et al., 2024). In this study, we focused on investigating the AF protein targets of nocuolin A in mussel plantigrades, based on its observed ability to inhibit settlement. A well-known pathway in the production of mussel biological adhesives (byssal threads) involves the 3,4-dihydroxyphenyl-L-alanine (L-DOPA) metabolism, which is crucial for the production of DOPA-containing byssal plaques. This process is catalyzed by the enzyme tyrosinase, which converts DOPA precursors into DOPA residues (Chen and Qian, 2017; Martín-Rodríguez et al., 2015). Additionally, certain molecules, such as the enzyme acetylcholinesterase (AChE), are affected by AF compound exposure in fouling organisms, as AChE is involved in cholinergic neural signalling during settlement (Chen and Qian, 2017). Two natural compounds isolated from marine organisms, territrem A and pulmonarin, were found to have AF activity associated with AChE inhibition (Nong et al., 2014; Tadesse et al., 2014). The commercial booster biocide Sea-Nine 211 also functions through this mechanism (Chen et al., 2014, 2017). Regarding compounds that act on the tyrosinase pathway, the cyclo-L-Trp-Ala, isolated from the sponge-associated fungus *Eurotium chevalieri* MUT 2316, was found to exert its AF activity via tyrosinase inhibition (Bovio et al., 2019). However, our results suggested that nocuolin A AF activity may not involve these metabolic pathways, as no modulation was found for either enzyme *in vitro*. Characterizing the molecular targets of AF compounds through untargeted shotgun proteomics is a complex process particularly when performed in non-model organisms such as the case of the mussel *M. galloprovincialis*. The absence of annotated genomes in the available databases used by gene set enrichment analysis online programs implies using homologous sequences from other represented organisms, namely the oyster *Crassostrea gigas*. Despite the similarities, differences in adhesion mechanisms among species may result in an imperfect representation of the mussel adhesive proteins in gene set enrichment. Nonetheless, untargeted shotgun proteomics was performed on mussel plantigrades exposed to nocuolin A. Of the 1718 proteins, only precollagen NG and precollagen D were found to be related to mussel adhesive proteins. These prepolymerized collagens (preCOLs), secreted by the collagen gland located on the mussel foot, are core components of the byssal threads (Waite et al., 1998). Depending on their distribution along the thread, the preCOLs are classified as distal (preCOL-D), connected to the byssal plaque, non-gradient (preCOL-NG), located at the center of the thread, and proximal (preCOL-P) found in the region closer to the mussel. The different preCOLs also confer different properties to the byssal thread. For example, preCOL-NG which grants resistance to pepsin digestion and mediates the interaction between the other two preCOLs, while preCOL-D, with its silk-fibroin domains, allows extensibility to the thread (Silverman and Roberto, 2007; Waite et al., 1998). Thus, alterations in these precollagens would greatly impair the efficiency of the byssal threads and, therefore, the adhesion of the mussel plantigrades to substrates. Nonetheless, despite being identified in the mussel plantigrades, none of these precollagens were considered differentially expressed in the samples exposed to nocuolin A compared to the control group, after applying the $\log_2$ fold change of 1.5 threshold. Of the proteins that were considered differently expressed when compared to the control ($\log_2$ fold change of 1.5), some were common to both concentrations of nocuolin A, while the majority were significantly altered by each concentration.

Proteins associated with basic biological processes such as vesicle transportation (coatomer subunit delta, and AP-2 complex subunit alpha) and eukaryotic translation complex (translation initiation factor 3 subunit A, eukaryotic translation initiation factor 3 subunit B) seemed to be upregulated by nocuolin A, at the concentration of 5 μM. The coatomer subunit delta is found in the Golgi apparatus, as part of the coatomer protein complex I (COPI), which is responsible for forming COPI-coated vesicles and the retrograde transport from the Golgi apparatus to the Endoplasmic Reticulum (ER), as well as transport within Golgi compartments (Beck et al., 2009). The AP-2 complex subunit alpha integrates the adaptor protein 2 (AP-2) complex and is involved in the formation of clathrin-coated vesicles, facilitating clathrin-mediated endocytosis (Traub, 2009). Vesicular carriers are fundamental for maintaining cellular homeostasis, and interferences in proteins associated with this process could lead to ER stress and disruption of cellular homeostasis. Eukaryotic translation initiation factors are essential for translation start site specificity, facilitating the assembly of the ribosome on the mRNA, and/or being involved in the hydrolysis of GTP for energy production during ribosomal assembly

(Sonenberg and Dever, 2003). Alterations in these translation factors could reflect cellular stress, impairing protein synthesis and, therefore, overall cellular function. At the higher concentration, nocuolin A seemed to alter proteins associated with muscle contraction (troponin T, myosin regulatory light chain, and myosin-XV) and mitochondrial function (cytochrome *c* oxidase subunit 5A, calcium-binding mitochondrial carrier protein SCaMC-2 and succinate dehydrogenase). Troponin T is one of the three subunits that comprise the troponin complex, along with troponin I and troponin C, which exhibit similar functions to their vertebrate homologous proteins, albeit with structural differences (Hooper et al., 2008; Inoue et al., 1996; Lehman, 1981). The troponin complex, found in the striated muscle of the adductor muscle on mussels, is a key regulatory protein on muscle contraction that initiates with the binding of Ca^{2+} (Funabara et al., 2013). The myosin subunit, myosin regulatory light chain, is found on smooth muscle fibres of the muscle foot, where it regulates myosin contractile activity (Katoh et al., 2002). Downregulation of muscle regulation proteins could lead to an overall dysfunctional muscle activity. If the mussels' foot muscle function were compromised, the adhesion process could be undermined, as mussel adhesion proteins are synthesized, secreted, and modulated by the mussel foot (DeMartini et al., 2017). Both succinate dehydrogenase and cytochrome *c* oxidase are involved in the electron transport chain on the mitochondrial inner membrane (as complex II and complex IV respectively), which is essential for ATP synthesis (Osellame et al., 2012). The calcium-binding mitochondrial carrier protein SCaMC-2 is a mitochondrial transporter of ATP-Mg/Pi responsible for ADP/ATP transport, calcium binding, and regulation of mitochondrial bioenergetics regulation (del Arco et al., 2016; Satrústegui et al., 2007). Overexpression of these proteins could impair ATP production and promote oxidative stress and metabolic dysregulation, consistent with a general cytotoxicity/ROS mode of action. Previous findings describe nocuolin A's activity in cancer cell lines as a promoter of ER stress, as shown by increased expression of the *p*-EIF2α protein, and as a disruptor of bioenergetic balance by reducing cellular ATP levels (Sousa et al., 2019), which aligns with our findings in mussel plantigrades. Moreover, other AF compounds have been shown to modulate ATPase activity, although via different pathways, suggesting that bioenergetic metabolism modulation may be a common mechanism of action among AF agents (Antunes et al., 2019; Dash et al., 2012; Han et al., 2013, Qian et al., 2010a,b; Zhang et al., 2012). Overall, the results of this study suggest that nocuolin A's AF activity in mussel plantigrades likely results from interference with vesicle transportation, mitochondrial ATP production, and muscle regulation. These general targets appear to reflect a global stress response in the mussel to the stress induced by nocuolin A, categorizing its mode of action as a protein expression regulator, as observed with other natural compounds (Antunes et al., 2019; Dash et al., 2012; Han et al., 2013; Oliveira et al., 2016).

New AF compounds should also have a minimal impact on the environment, in addition to preventing the attachment and/or growth of fouling organisms. In this work, the toxicity of nocuolin A was studied in both target and non-target organisms. For target organisms, the therapeutic ratio (LC_{50}/EC_{50}) higher than 15 was used to assess the effectiveness of the compound relative to its toxicity, recognizing that these are working values and not absolutes (Rittschof et al., 2003). No mortality was observed in the five biofilm-forming marine bacteria or the mussel plantigrades when exposed to the compound at tested concentrations. Furthermore, in the mussel plantigrades, nocuolin A displayed an $LC_{50} > 29.843$ μg mL^{-1} and a therapeutic value higher than 15 (LC_{50}/EC_{50} value of 25.61). However, toxicity was observed in other target species, including *Navicula* sp. ($LC_{50} > 0.925$ μg mL^{-1} and $LC_{50}/EC_{50} = 1.986$) and *A. amphitrite* nauplii ($LC_{50} = 0.00483$ μg mL^{-1}), as wells as non-target marine and freshwater organisms represented by *A. salina* nauplii ($LC_{50} = 0.740$ μg mL^{-1}) and *D. rerio* embryos ($LC_{50} = 0.0174$ μg mL^{-1}). A similar profile was observed for the compound portimine, which was isolated from the dinoflagellate *Vulcanodinium rugosum*, towards macrofouling species larvae (*M. galloprovinciallis* D-veliger and *A. improvisus* cyprids), where larval development and metamorphosis were inhibited via apoptosis (Brooke et al., 2018). The same mechanism could be responsible for the toxicity observed in *A. amphitrite* nauplii, since apoptosis induction has already been described as nocuolin A's mode of action on colon cancer cells in both monolayer and spheroid cultures (Sousa et al., 2019). Moreover, since the mussel plantigrades are at a later developmental stage and are more robust than D-veliger and barnacle nauplii, this could also explain the resistance of the plantigrades to the compound. The furanone derivatives omF1 and omF2, isolated from *Streptomycetes violaceoruber* SCH-09, were also active but non-toxic towards *Navicula annexa* ($LC_{50}/EC_{50} = 173–290$, respectively), and *A. salina* ($LC_{50} = 118.9–81.9$ μg mL^{-1}, respectively) (Hong and Cho, 2013). These values were far higher than those obtained for nocuolin A, confirming the high toxicity of our compound towards these organisms. Another example is the AF compound maculalactone A, isolated from the cyanobacteria *Kyrtuthrix maculans*, which was found to be toxic to the larvae of various barnacles' species ($LC_{50} = 1.1–5.2$ μg mL^{-1}) and to *A. salina* nauplii ($LC_{50} = 3.7$ μg mL^{-1}) (Brown et al., 2004). Nonetheless, our LC_{50} values for the same organisms were even lower. In fact, the toxicity exerted by nocuolin A was most comparable to that of already-known biocides, such as Irgarol 1051 ($LC_{50}/EC_{50} = 6$ for *Navicula annexa* and $LC_{50} = 0.51$ μg mL^{-1} for *A. salina*) (Hong and Cho, 2013) and tralopyril ($LC_{50} = 0.00502$ μg mL^{-1} for *D. rerio* embryos) (Oliveira et al., 2017). These results highlighted the toxicity of our compound towards several organisms, including the early development stages of a target macrofouling species, which delays its potential as an environmentally compatible AF agent. An example of a compound with low risk is capsaicin, the natural chilli pepper extract that has been commonly used as an animal repellent (EPA, 1992). Studies suggest that the risk of capsaicin as an AF biocide is relatively low for the marine environment (Oliveira et al., 2014, 2017; Wang et al., 2014) and based on degradation, bioaccumulation, toxicity and accumulation in sediments, additional studies may not be necessary (Wang et al., 2014). Since then, other compounds inspired by capsaicin's structure have emerged (An et al., 2022; Wang et al., 2020, 2022). Nocuolin A, on the other hand, raises some concerns regarding some of the parameters analyzed, including the risk characterization that indicates a potential threat to the environment. However, essential information, such as the compound's half-life and persistence, is still missing. Conducting such studies early may help avoid future problems, as the history of AF usage is full of examples of environmentally friendly compounds later found to be harmful. Thus, a potential path could involve structural optimization of nocuolin A into less toxic analogues, especially for non-target organisms, while maintaining its bioactivity against fouling organisms (Liu et al., 2020). Following this lead, and after chemical optimization, future work should also include a broader screening of AF activity against other important macrofouling species (Vinagre et al., 2020), to provide a more comprehensive AF profile of the compounds.

5. Conclusions

This study explored the biotechnological potential of nocuolin A as an AF agent by investigating its activity against organisms at different levels of biological organization, identifying molecular targets in *M. galloprovincialis* plantigrades, and assessing its overall environmental toxicity and risk. Nocuolin A effectively inhibited the settlement of plantigrade mussel post-larvae without demonstrating toxicity towards this species. The molecular targets of this AF activity appear to involve alterations in mitochondrial energetic metabolism (cytochrome *c* oxidase, calcium-binding mitochondrial carrier protein SCaMC-2, and succinate dehydrogenase) and muscle regulation (troponin T), through the upregulation of these proteins. Additionally, nocuolin A successfully inhibited the growth of *Navicula* sp. However, despite its broad-spectrum AF activity against both micro and macrofouling organisms, nocuolin A exhibited high toxicity toward the marine biofilm-forming

diatoms, barnacle larvae, and non-target organisms, such as *A. salina* and *D. rerio*. The simulations of environmental nocuolin A concentrations, combined with ecotoxicity results, suggest a significant ecological risk. Given that environmentalcompatibility is a key requirement for new compounds to be integrated into AF technologies, nocuolin A's toxicity limits its immediate potential. Further research, including structure optimization and structure-activity relationship (SAR) studies, may help to identify less toxic analogues that retain AF activity while minimizing environmental risks.

Funding

This research was supported by national funds through FCT (Portuguese Foundation for Science and Technology) within the strategic fund (UIDB/04423/2020 and UIDP/04423/2020) and the project PTDC/CTA-AMB/0853/2021. This work was supported by the Innovation Pact, Project No. C644915664-00000026 (WP2 Vertical Bivalves), under the "Blue Bioeconomy Pact", resulting from the submission of the application to Notice No. 02/C05-i01/2022, within the scope of the Recovery and Resilience Plan (PRR), co-funded by the Portuguese Republic and the European Union. FCT supported SP (https://doi.org/10.54499/SFRH/BD/145380/2019) and CG (2022.12028.BD) through PhD grants, and IBO and JRA for work contracts through the Scientific Employment Stimulus Individual Call (https://doi.org/10.54499/CEECIND/01368/2018/CP1574/CT0005 and https://doi.org/10.54499/2022.03876.CEECIND/CP1728/CT0005, respectively).

CRediT authorship contribution statement

Sandra Pereira: Writing – original draft, Methodology, Investigation, Formal analysis, Data curation. **Isabel B. Oliveira:** Writing – review & editing, Validation, Methodology, Investigation, Formal analysis, Data curation. **Maria Lígia Sousa:** Writing – review & editing, Validation, Investigation. **Catarina Gonçalves:** Writing – review & editing, Investigation, Formal analysis. **Marco Preto:** Writing – review & editing, Validation. **Maria V. Turkina:** Writing – review & editing, Validation, Methodology, Investigation. **Vitor Vasconcelos:** Writing – review & editing, Validation, Supervision, Resources, Investigation. **Alexandre Campos:** Writing – review & editing, Validation, Supervision, Methodology, Funding acquisition. **Joana R. Almeida:** Writing – review & editing, Validation, Supervision, Resources, Project administration, Methodology, Investigation, Funding acquisition, Conceptualization.

Declaration of competing interest

The authors declare the following financial interests/personal relationships which may be considered as potential competing interests:

Joana R. Almeida reports was provided by Foundation for Science and Technology. Joana R. Almeida reports financial support was provided by European Union. If there are other authors, they declare that they have no known competing financial interests or personal relationships that could have appeared to influence the work reported in this paper.

Data availability

Data will be made available on request.

Acknowledgements

The authors thank the Blue Biotechnology and Ecotoxicology Culture Collection (LEGE-CC) at CIIMAR (https://lege.ciimar.up.pt) for their support.

Appendix A. Supplementary data

Supplementary data to this article can be found online at https://doi.org/10.1016/j.chemosphere.2024.143318.

References

Adhikari, A., Devkota, H.P., Takano, A., Masuda, K., Nakane, T., Basnet, P., Skalko-Basnet, N., 2008. Screening of Nepalese crude drugs traditionally used to treat hyperpigmentation: in vitro tyrosinase inhibition. Int. J. Cosmet. Sci. 30 (5), 353–360. https://doi.org/10.1111/j.1468-2494.2008.00463.x.

Alfaro, A.C., Jeffs, A.G., Creese, R.G., 2004. Bottom-drifting algal/mussel spat associations along a sandy coastal region in northern New Zealand. Aquaculture 241 (1–4), 269–290. https://doi.org/10.1016/j.aquaculture.2004.07.029.

Almeida, J.R., Correia-Da-Silva, M., Sousa, E., Antunes, J., Pinto, M., Vasconcelos, V., Cunha, I., 2017. Antifouling potential of Nature-inspired sulfated compounds. Sci. Rep. 7 (January), 1–11. https://doi.org/10.1038/srep42424.

Almeida, J.R., Freitas, M., Cruz, S., Leão, P.N., Vasconcelos, V., Cunha, I., 2015. Acetylcholinesterase in biofouling species: characterization and mode of action of cyanobacteria-derived antifouling agents. Toxins 7 (8), 2739–2756. https://doi.org/10.3390/toxins7082739.

Almeida, J.R., Moreira, J., Pereira, D., Pereira, S., Antunes, J., Palmeira, A., Vasconcelos, V., Pinto, M., Correia-Da-Silva, M., Cidade, H., 2018. Potential of synthetic chalcone derivatives to prevent marine biofouling. Sci. Total Environ. 643, 98–106. https://doi.org/10.1016/j.scitotenv.2018.06.169.

Almeida, J.R., Vasconcelos, V., 2015. Natural antifouling compounds: effectiveness in preventing invertebrate settlement and adhesion. Biotechnol. Adv. 33 (3–4), 343–357. https://doi.org/10.1016/j.biotechadv.2015.01.013.

An, X., Yang, X., Dong, W., Ni, C., Jiang, X., Li, X., 2022. Synthesis and fouling resistance of capsaicin derivatives containing amide groups. Chem. Phys. Lett. 803 (March), 139824 https://doi.org/10.1016/j.cplett.2022.139824.

Antunes, J., Pereira, S., Ribeiro, T., Plowman, J.E., Thomas, A., Clerens, S., Campos, A., Vasconcelos, V., Almeida, J.R., 2019. A multi-bioassay integrated approach to assess the antifouling potential of the cyanobacterial metabolites portoamides. Mar. Drugs 17 (2), 1–19. https://doi.org/10.3390/md17020111.

Bateman, A., Martin, M.J., Orchard, S., Magrane, M., Ahmad, S., Alpi, E., Bowler-Barnett, E.H., Britto, R., Bye-A-Jee, H., Cukura, A., Denny, P., Dogan, T., Ebenezer, T. G., Fan, J., Garmiri, P., da Costa Gonzales, L.J., Hatton-Ellis, E., Hussein, A., Ignatchenko, A., et al., 2023. UniProt: the universal protein Knowledgebase in 2023. Nucleic Acids Res. 51 (D1), D523–D531. https://doi.org/10.1093/nar/gkac1052.

Beck, R., Ravet, M., Wieland, F.T., Cassel, D., 2009. The COPI system: molecular mechanisms and function. FEBS (Fed. Eur. Biochem. Soc.) Lett. 583 (17), 2701–2709. https://doi.org/10.1016/j.febslet.2009.07.032.

Bovio, E., Fauchon, M., Toueix, Y., Mehiri, M., Varese, G.C., Hellio, C., 2019. The sponge-associated fungus Eurotium chevalieri MUT 2316 and its bioactive molecules: potential applications in the field of antifouling. Mar. Biotechnol. 21 (6), 743–752. https://doi.org/10.1007/s10126-019-09920-y.

Brooke, D.G., Cervin, G., Champeau, O., Harwood, D.T., Pavia, H., Selwood, A.I., Svenson, J., Tremblay, L.A., Cahill, P.L., 2018. Antifouling activity of portimine, select semisynthetic analogues, and other microalga-derived spirocyclic imines. Biofouling 34 (8), 950–961. https://doi.org/10.1080/08927014.2018.1514461.

Brown, G.D., Wong, H.F., Hutchinson, N., Lee, S.C., Chan, B.K.K., Williams, G.A., 2004. Chemistry and biology of maculalactone A from the marine cyanobacterium Kyrtuthrix maculans. Phytochemistry Rev. 3 (3), 381–400. https://doi.org/10.1007/s11101-004-6552-5.

Cahill, P.L., Moodie, L.W.K., Hertzer, C., Pinori, E., Pavia, H., Hellio, C., Brimble, M.A., Svenson, J., 2024. Creating new antifoulants using the tools and tactics of medicinal chemistry. Accounts of Chemical Research 57 (3), 399–412. https://doi.org/10.1021/acs.accounts.3c00733.

Campos, A., Danielsson, G., Farinha, A.P., Kuruvilla, J., Warholm, P., Cristobal, S., 2016. Shotgun proteomics to unravel marine mussel (Mytilus edulis) response to long-term exposure to low salinity and propranolol in a Baltic Sea microcosm. J. Proteonomics 137, 97–106. https://doi.org/10.1016/j.jprot.2016.01.010.

Carl, C., Poole, A.J., Vucko, M.J., Williams, M.R., Whalan, S., de Nys, R., 2011. Optimising settlement assays of pediveligers and plantigrades of Mytilus galloprovincialis. Biofouling 27 (8), 859–868. https://doi.org/10.1080/08927014.2011.605943.

Chen, L., Au, D.W.T., Hu, C., Peterson, D.R., Zhou, B., Qian, P.Y., 2017. Identification of molecular targets for 4,5-Dichloro-2-n-octyl-4-isothiazolin-3-one (DCOIT) in teleosts: new insight into mechanism of toxicity. Environ. Sci. Technol. 51 (3), 1840–1847. https://doi.org/10.1021/acs.est.6b05523.

Chen, L., Qian, P.Y., 2017. Review on molecular mechanisms of antifouling compounds: an update since 2012. Mar. Drugs 15 (9), 1–20. https://doi.org/10.3390/md15090264.

Chen, L., Zhang, H., Sun, J., Wong, Y.H., Han, Z., Au, D.W.T., Bajic, V.B., Qian, P.Y., 2014. Proteomic changes in brain tissues of marine medaka (Oryzias melastigma) after chronic exposure to two antifouling compounds: butenolide and 4,5-dichloro-2-n-octyl-4-isothiazolin-3-one (DCOIT). Aquat. Toxicol. 157, 47–56. https://doi.org/10.1016/j.aquatox.2014.09.010.

Chmelík, D., Hrouzek, P., Fedorko, J., Long, D., Urajová, P., Mare, J., Jan, Č., 2019. Accumulation of Cyanobacterial Oxadiazine Nocuolin A Is Enhanced by Temperature Shift during Cultivation and Is Promoted by Bacterial Co- Habitants in the Culture, vol. 44. https://doi.org/10.1016/j.algal.2019.101673. September.

Conesa, A., Götz, S., 2008. Blast2GO: a comprehensive suite for functional analysis in plant genomics. Int. J. Plant Genom. 2008 https://doi.org/10.1155/2008/619832.
Conesa, A., Götz, S., García-Gómez, J.M., Terol, J., Talón, M., Robles, M., 2005. Blast2GO: a universal tool for annotation, visualization and analysis in functional genomics research. Bioinformatics 21 (18), 3674–3676. https://doi.org/10.1093/bioinformatics/bti610.
Dahms, H.U., Ying, X., Pfeiffer, C., 2006. Antifouling potential of cyanobacteria: a mini-review. Biofouling 22 (5), 317–327. https://doi.org/10.1080/08927010600967261.
Dash, S., Chandramouli, K.H., Zhang, Y., Qian, P.Y., 2012. Effects of poly-ether B on proteome and phosphoproteome expression in biofouling Balanus amphitrite cyprids. Biofouling 28 (4), 405–415. https://doi.org/10.1080/08927014.2012.679731.
del Arco, A., Contreras, L., Pardo, B., Satrustegui, J., 2016. Calcium regulation of mitochondrial carriers. Biochimica et Biophysica Acta - Molecular Cell Research 1863 (10), 2413–2421. https://doi.org/10.1016/j.bbamcr.2016.03.024.
DeMartini, D.G., Errico, J.M., Sjoestroem, S., Fenster, A., Waite, J.H., 2017. A cohort of new adhesive proteins identified from transcriptomic analysis of mussel foot glands. Journal of the Royal Society Interface 14 (131). https://doi.org/10.1098/rsif.2017.0151.
Ellman, G.L., Courtney, K.D., Andres, V., Featherstone, R.M., 1961. A new and rapid colorimetric determination of acetylcholinesterase activity. In: Biochemical Pharmacology, vol. 7. Pergamon Press Ltd.
European Commission, 2003. Technical Guidance Document on Risk Assessment, pp. 1–337.
European Commission, & European Climate Infrastructure and Environment Executive Agency, 2021. Sustainability criteria for the blue economy : main report (Issue March). https://data.europa.eu/doi/10.2826/399476.
Figueiredo, S.A.C., Preto, M., Moreira, G., Martins, T.P., Abt, K., Melo, A.Ø., Vasconcelos, V.M., Le, P.N., 2021. Natural Products Discovery Discovery of Cyanobacterial Natural Products Containing Fatty Acid Residues, pp. 10152–10160. https://doi.org/10.1002/ange.202015105.
Funabara, D., Watanabe, D., Satoh, N., Kanoh, S., 2013. Genome-wide survey of genes encoding muscle proteins in the pearl oyster, Pinctada fucata. Zool. Sci. 30 (10), 817–825. https://doi.org/10.2108/zsj.30.817.
Gimeno, S., Allan, D., Kai, P., Remuzat, P., Collard, M., 2024. Are current regulatory log Kow cut-off values fit-for-purpose as a screening tool for bioaccumulation potential in aquatic organisms? Regul. Toxicol. Pharmacol. 147 (July 2023) https://doi.org/10.1016/j.yrtph.2023.105556.
Götz, S., García-Gómez, J.M., Terol, J., Williams, T.D., Nagaraj, S.H., Nueda, M.J., Robles, M., Talón, M., Dopazo, J., Conesa, A., 2008. High-throughput functional annotation and data mining with the Blast2GO suite. Nucleic Acids Res. 36 (10), 3420–3435. https://doi.org/10.1093/nar/gkn176.
Grandič, M., Zovko, A., Frangež, R., Turk, T., Sepčić, K., 2012. Binding and permeabilization of lipid bilayers by natural and synthetic 3-alkylpyridinium polymers. Bioorg. Med. Chem. 20 (5), 1659–1664. https://doi.org/10.1016/j.bmc.2012.01.027.
Han, Z., Sun, J., Zhang, Y., He, F., Xu, Y., Matsumura, K., He, L.S., Qiu, J.W., Qi, S.H., Qian, P.Y., 2013. ITRAQ-based proteomic profiling of the barnacle Balanus amphitrite in response to the antifouling compound meleagrin. J. Proteome Res. 12 (5), 2090–2100. https://doi.org/10.1021/pr301083e.
Hanssen, K., Cervin, G., Trepos, R., Petitbois, J., Haug, T., Hansen, E., Andersen, J.H., Pavia, H., Hellio, C., Svenson, J., 2014. The bromotyrosine derivative ianthelline isolated from the arctic marine sponge stryphnus fortis inhibits marine micro- and macrobiofouling. Mar. Biotechnol. 16 (6), 684–694. https://doi.org/10.1007/s10126-014-9583-y.
Hong, Y.K., Cho, J.Y., 2013. Effect of seaweed epibiotic bacterium Streptomyces violaceoruber SCH-09 on marine fouling organisms. Fisheries Science 79 (3), 469–475. https://doi.org/10.1007/s12562-013-0604-y.
Hooper, S.L., Hobbs, K.H., Thuma, J.B., 2008. Invertebrate muscles: thin and thick filament structure; molecular basis of contraction and its regulation, catch and asynchronous muscle. Progress in Neurobiology 86 (2), 72–127. https://doi.org/10.1016/j.pneurobio.2008.06.004.
Inoue, A., Ojima, T., Nishita, K., 1996. Cloning and sequencing of a cDNA for Akazara scallop troponin T. J. Biochem. 120 (4), 834–837. https://doi.org/10.1093/oxfordjournals.jbchem.a021487.
Käll, L., Storey, J.D., Noble, W.S., 2008. Non-parametric estimation of posterior error probabilities associated with peptides identified by tandem mass spectrometry. Bioinformatics 24 (16), 42–48. https://doi.org/10.1093/bioinformatics/btn294.
Katoh, T., Konishi, K., Yazawa, M., 2002. Essential light chain modulates phosphorylation-dependent regulation of smooth muscle myosin. J. Biochem. 131 (5), 641–645. https://doi.org/10.1093/oxfordjournals.jbchem.a003146.
Kolberg, L., Raudvere, U., Kuzmin, I., Adler, P., Vilo, J., Peterson, H., 2023. G:Profiler-interoperable web service for functional enrichment analysis and gene identifier mapping (2023 update). Nucleic Acids Res. 51 (W1), W207–W212. https://doi.org/10.1093/nar/gkad347.
Labriere, C., Elumalai, V., Staffansson, J., Cervin, G., Le Norcy, T., Denardou, H., Réhel, K., Moodie, L.W.K., Hellio, C., Pavia, H., Hansen, J.H., Svenson, J., 2020. Phidianidine A and synthetic analogues as naturally inspired marine antifoulants. Journal of Natural Products 83 (11), 3413–3423. https://doi.org/10.1021/acs.jnatprod.0c00881.
Leão, P.N., Vasconcelos, M.T.S.D., Vasconcelos, V.M., 2009. Allelopathy in freshwater cyanobacteria. Crit. Rev. Microbiol. 35 (4), 271–282. https://doi.org/10.3109/10408410902823705.
Lehman, W., 1981. Thin-filament-like regulation in molluscan muscles. Biochim. Biophys. Acta 668, 349–356.
Liu, L.L., Wu, C.H., Qian, P.Y., 2020. Marine natural products as antifouling molecules–a mini-review (2014–2020). Biofouling 36 (10), 1210–1226. https://doi.org/10.1080/08927014.2020.1864343.
Mabrouk, S.B., Reis, M., Sousa, M.L., Ribeiro, T., Almeida, J.R., Pereira, S., Antunes, J., Rosa, F., Vasconcelos, V., Achour, L., Kacem, A., Urbatzka, R., 2020. The marine seagrass halophila stipulacea as a source of bioactive metabolites against obesity and biofouling. Mar. Drugs 18 (2). https://doi.org/10.3390/md18020088.
Maeder, V., Escher, B.I., Scheringer, M., Hungerbühler, K., 2004. Toxic ratio as an indicator of the intrinsic toxicity in the assessment of persistent, bioaccumulative, and toxic chemicals. Environ. Sci. Technol. 38 (13), 3659–3666. https://doi.org/10.1021/es0351591.
Martín-Rodríguez, A.J., Babarro, J.M.F., Lahoz, F., Sansón, M., Martín, V.S., Norte, M., Fernández, J.J., 2015. From broad-spectrum biocides to quorum sensing disruptors and mussel repellents: antifouling profile of alkyl triphenylphosphonium salts. PLoS One 10 (4), 1–30. https://doi.org/10.1371/journal.pone.0123652.
Martins, T.P., Glasser, N.R., Kountz, D.J., Oliveira, P., Balskus, E.P., Lea, P.N., 2022. Biosynthesis of the unusual carbon skeleton of nocuolin A. https://doi.org/10.1021/acschembio.2c00464.
Nesvizhskii, A.I., Keller, A., Kolker, E., Aebersold, R., 2003. A statistical model for identifying proteins by tandem mass spectrometry. Anal. Chem. 75 (17), 4646–4658. https://doi.org/10.1021/ac0341261.
Neves, A.R., Vilas Boas, C., Gonçalves, C., Vasconcelos, V., Pinto, M., Silva, E.R., Sousa, E., Almeida, J.R., Correia-da-Silva, M., 2022. Gallic acid derivatives as inhibitors of mussel (Mytilus galloprovincialis) larval settlement: lead optimization, biological evaluation and use in antifouling coatings. Bioorg. Chem. 126 (May) https://doi.org/10.1016/j.bioorg.2022.105911.
Nong, X.H., Wang, Y.F., Zhang, X.Y., Zhou, M.P., Xu, X.Y., Qi, S.H., 2014. Territrem and butyrolactone derivatives from a marine-derived fungus aspergillus terreus. Mar. Drugs 12 (12), 6113–6124. https://doi.org/10.3390/md12126113.
OECD, 2004. OECD Environmental Health and Safety Publications Series on Emission Scenario Documents No . 10 EMISSION SCENARIO DOCUMENT on Environment Directorate Organisation for Economic Co-operation and Development December 2004, vol. 10, p. 119.
OECD, 2013. Test No. 236: fish embryo acute toxicity (FET) test. In: OECD Guidelines for the Testing of Chemicals, Section 2. OECD Publishing, pp. 1–22. July. http://www.oecd-ilibrary.org.
Oliveira, I.B., Beiras, R., Thomas, K.V., Suter, M.J.F., Barroso, C.M., 2014. Acute toxicity of tralopyril, capsaicin and triphenylborane pyridine to marine invertebrates. Ecotoxicology 23 (7), 1336–1344. https://doi.org/10.1007/s10646-014-1276-9.
Oliveira, I.B., Groh, K.J., Schönenberger, R., Barroso, C., Thomas, K.V., Suter, M.J.F., 2017. Toxicity of emerging antifouling biocides to non-target freshwater organisms from three trophic levels. Aquat. Toxicol. 191 (January), 164–174. https://doi.org/10.1016/j.aquatox.2017.07.019.
Oliveira, I.B., Groh, K.J., Stadnicka-Michalak, J., Schönenberger, R., Beiras, R., Barroso, C.M., Langford, K.H., Thomas, K.V., Suter, M.J.F., 2016. Tralopyril bioconcentration and effects on the gill proteome of the Mediterranean mussel Mytilus galloprovincialis. Aquat. Toxicol. 177, 198–210. https://doi.org/10.1016/j.aquatox.2016.05.026.
Osellame, L.D., Blacker, T.S., Duchen, M.R., 2012. Cellular and molecular mechanisms of mitochondrial function. Best Pract. Res. Clin. Endocrinol. Metabol. 26 (6), 711–723. https://doi.org/10.1016/j.beem.2012.05.003.
Paz-Villarraga, C.A., Castro, Í.B., Fillmann, G., 2022. Biocides in antifouling paint formulations currently registered for use. Environ. Sci. Pollut. Control Ser. 30090–30101. https://doi.org/10.1007/s11356-021-17662-5.
Pereira, D., Almeida, J.R., Cidade, H., Correia-da-silva, M., 2024. Proof of Concept of Natural and Synthetic Antifouling Agents in Coatings, vols. 1–26.
Pereira, F., Almeida, J.R., Paulino, M., Grilo, I.R., Macedo, H., Cunha, I., Sobral, R.G., Vasconcelos, V., Gaudêncio, S.P., 2020. Antifouling napyradiomycins from marine-derived actinomycetes streptomyces aculeolatus. Mar. Drugs 18 (1), 1–19. https://doi.org/10.3390/md18010063.
Pérez, M., García, M., Ruiz, D., Autino, J.C., Romanelli, G., Blustein, G., 2016. Antifouling activity of green-synthesized 7-hydroxy-4-methylcoumarin. Mar. Environ. Res. 113, 134–140. https://doi.org/10.1016/j.marenvres.2015.11.010.
Pérez, V.T., Ticona, L.A., Cabanillas, A.H., Corral, S.M., Fernando, D., Valencia, R., Quintana, A.M., Rumbero, Á., 2023. Isolation of nocuolin A and synthesis of new oxadiazine derivatives. Design , Synthesis , Molecular Docking. Apoptotic.
Petitbois, J.G., Casalme, L.O., Lopez, J.A.V., Alarif, W.M., Abdel-Lateff, A., Al-Lihaibi, S. S., Yoshimura, E., Nogata, Y., Umezawa, T., Matsuda, F., Okino, T., 2017. Serinolamides and lyngbyabellins from an Okeania sp. cyanobacterium collected from the red Sea. Journal of Natural Products 80 (10), 2708–2715. https://doi.org/10.1021/acs.jnatprod.7b00449.
Piazza, V., Ferioli, A., Giacco, E., Melchiorre, N., Valenti, A., Del Prete, F., Biandolino, F., Dentone, L., Frisenda, P., Faimali, M., 2012. A standardization of Amphibalanus (Balanus) amphitrite (Crustacea, Cirripedia) larval bioassay for ecotoxicological studies. Ecotoxicol. Environ. Saf. 79, 134–138. https://doi.org/10.1016/j.ecoenv.2011.12.014.
Qian, P.Y., Cheng, A., Wang, R., Zhang, R., 2022. Marine biofilms: diversity, interactions and biofouling. Nat. Rev. Microbiol. 20 (11), 671–684. https://doi.org/10.1038/s41579-022-00744-7.
Qian, P.Y., Wong, Y.H., Zhang, Y., 2010a. Changes in the proteome and phosphoproteome expression in the bryozoan Bugula neritina larvae in response to the antifouling agent butenolide. Proteomics 10 (19), 3435–3446. https://doi.org/10.1002/pmic.201000199.
Qian, P.Y., Xu, Y., Fusetani, N.N.N., 2010b. Natural products as antifouling compounds: recent progress and future perspectives. Biofouling 26 (2), 223–234. https://doi.org/10.1080/08927010903470815.

Ramos, V., Morais, J., Castelo-Branco, R., Pinheiro, Â., Martins, J., Regueiras, A., Pereira, A.L., Lopes, V.R., Frazão, B., Gomes, D., Moreira, C., Costa, M.S., Brûle, S., Faustino, S., Martins, R., Saker, M., Osswald, J., Leão, P.N., Vasconcelos, V.M., 2018. Cyanobacterial diversity held in microbial biological resource centers as a biotechnological asset: the case study of the newly established LEGE culture collection. J. Appl. Phycol. 30 (3), 1437–1451. https://doi.org/10.1007/s10811-017-1369-y.

Resende, D.I.S.P., Almeida, J.R., Pereira, S., Campos, A., Lemos, A., Plowman, J.E., Thomas, A., Clerens, S., Vasconcelos, V., Pinto, M., Correia-Da-silva, M., Sousa, E., 2021. From natural xanthones to synthetic C-1 aminated 3,4-dioxygenated xanthones as optimized antifouling agents. Mar. Drugs 19 (11). https://doi.org/10.3390/md19110638.

Rittschof, D., Clare, A.S., Gerhart, D.J., Mary, S.A., Bonaventura, J., 1992. Barnacle in vitro assays for biologically active substances: toxicity and settlement inhibition assays using mass cultured balanus amphitrite amphitrite Darwin. Biofouling 6 (2), 115–122. https://doi.org/10.1080/08927019209386217.

Rittschof, Dan, Lai, C.H., Kok, L.M., Teo, S.L.M., 2003. Pharmaceuticals as antifoulants: concept and principles. Biofouling 19, 207–212. https://doi.org/10.1080/0892701021000083769. Suppl. L.

Satrústegui, J., Pardo, B., Del Arco, A., 2007. Mitochondrial transporters as novel targets for intracellular calcium signaling. Physiol. Rev. 87 (1), 29–67. https://doi.org/10.1152/physrev.00005.2006.

Scholz, B., Liebezeit, G., 2012. Screening for competition effects and allelochemicals in benthic marine diatoms and cyanobacteria isolated from an intertidal flat (southern North Sea). Phycologia 51 (4), 432–450. https://doi.org/10.2216/11-80.1.

Schultz, M.P., Bendick, J.A., Holm, E.R., Hertel, W.M., 2011. Economic impact of biofouling on a naval surface ship. Biofouling 27 (1), 87–98. https://doi.org/10.1080/08927014.2010.542809.

Shannon, P., Markiel, A., Ozier, O., Baliga, N.S., Wang, J.T., Ramage, D., Amin, N., Schwikowski, B., Ideker, T., 2003. Cytoscape: a software Environment for integrated models of biomolecular interaction networks. Genome Res. 13 (11), 2498–2504. https://doi.org/10.1101/gr.1239303.

Silverman, H.G., Roberto, F.F., 2007. Understanding marine mussel adhesion. Mar. Biotechnol. 9 (6), 661–681. https://doi.org/10.1007/s10126-007-9053-x.

Sonenberg, N., Dever, T.E., 2003. Eukaryotic translation initiation factors and regulators. Curr. Opin. Struct. Biol. 13 (1), 56–63. https://doi.org/10.1016/S0959-440X(03)00009-5.

Sousa, M.L., Preto, M., Vasconcelos, V., Linder, S., Urbatzka, R., 2019. Antiproliferative effects of the natural oxadiazine nocuolin A are associated with impairment of mitochondrial oxidative phosphorylation. Front. Oncol. 9 (APR), 1–13. https://doi.org/10.3389/fonc.2019.00224.

Tadesse, M., Svenson, J., Sepčić, K., Trembleau, L., Engqvist, M., Andersen, J.H., Jaspars, M., Stensvaìšg, K., Haug, T., 2014. Isolation and synthesis of pulmonarins A and B, acetylcholinesterase inhibitors from the colonial ascidian Synoicum pulmonaria. Journal of Natural Products 77 (2), 364–369. https://doi.org/10.1021/np401002s.

Tan, L.T., Goh, B.P.L., Tripathi, A., Lim, M.G., Dickinson, G.H., Lee, S.S.C., Teo, S.L.M., 2010. Natural antifoulants from the marine cyanobacterium Lyngbya majuscula. Biofouling 26 (6), 685–695. https://doi.org/10.1080/08927014.2010.508343.

Team, R.C., 2021. R: A Language and Environment for Statistical Computing. R Foundation for Statistical Computing. https://www.r-project.org/.

Traub, L.M., 2009. Tickets to ride: selecting cargo for clathrin-regulated internalization. Nat. Rev. Mol. Cell Biol. 10 (9), 583–596. https://doi.org/10.1038/nrm2751.

US EPA, 2016. Estimation Programs Interface SuiteTM for Microsoft® Windows (4.11). United States Environmental Protection Agency.

Van Hattum, B., Baart, A., Boon, J., 2006. Emission estimation and chemical fate modelling of antifoulants. Handb. Environ. Chem. 5 (PART O), 101–120. https://doi.org/10.1007/698-5-051. Water Pollution, 5.

Vilas-Boas, C., Carvalhal, F., Pereira, B., Carvalho, S., Sousa, E., Pinto, M.M.M., Calhorda, M.J., Vasconcelos, V., Almeida, J.R., Silva, E.R., Correia-Da-Silva, M., 2020. One step forward towards the development of eco-friendly antifouling coatings: immobilization of a sulfated marine-inspired compound. Mar. Drugs 18 (10). https://doi.org/10.3390/md18100489.

Vilas-Boas, C., Neves, A.R., Carvalhal, F., Pereira, S., Calhorda, M.J., Vasconcelos, V., Pinto, M., Sousa, E., Almeida, J.R., Silva, E.R., Correia-da-Silva, M., 2021. Multidimensional characterization of a new antifouling xanthone: structure-activity relationship, environmental compatibility, and immobilization in marine coatings. Ecotoxicol. Environ. Saf. 228 https://doi.org/10.1016/j.ecoenv.2021.112970.

Vinagre, P.A., Simas, T., Cruz, E., Pinori, E., Svenson, J., 2020. Marine biofouling: a European database for the marine renewable energy sector. J. Mar. Sci. Eng. 8 (8) https://doi.org/10.3390/JMSE8070495.

Voráčová, K., Hájek, J., Mareš, J., Urajová, P., Kuzma, M., Cheel, J., Villunger, A., Kapuscik, A., Bally, M., Novák, P., Kabeláč, M., Krumschnabel, G., Lukeš, M., Voloshko, L., Kopecký, J., Hrouzek, P., 2017. The cyanobacterial metabolite nocuolin A is a natural oxadiazine that triggers apoptosis in human cancer cells. PLoS One 12 (3), 1–20. https://doi.org/10.1371/journal.pone.0172850.

Waite, H., Qin, X.-X., Coyne, K.3., 1998. The pecutiar collagens of mussel byssus. Matrix Biol. 17, 93–106.

Wang, J., Shi, T., Yang, X., Han, W., Zhou, Y., 2014. Environmental risk assessment on capsaicin used as active substance for antifouling system on ships. Chemosphere 104, 85–90. https://doi.org/10.1016/j.chemosphere.2013.10.061.

Wang, W.X., 2016. Bioaccumulation and biomonitoring. In: Marine Ecotoxicology: Current Knowledge and Future Issues. Elsevier Inc. https://doi.org/10.1016/B978-0-12-803371-5.00004-7.

Wang, X., Liu, Z., Jiang, X., Yu, L., 2022. Self-polishing antifouling coatings based on benzamide derivatives containing capsaicin. Mar. Pollut. Bull. 181 (April), 113844 https://doi.org/10.1016/j.marpolbul.2022.113844.

Wang, X., Yu, L., Liu, Y., Jiang, X., 2020. Synthesis and fouling resistance of capsaicin derivatives containing amide groups. Sci. Total Environ. 710, 136361 https://doi.org/10.1016/j.scitotenv.2019.136361.

Wiśniewski, J.R., Zougman, A., Nagaraj, N., Mann, M., 2009. Universal sample preparation method for proteome analysis. Nat. Methods 6 (5), 359–362. https://doi.org/10.1038/nmeth.1322.

Wissner, J.L., Almeida, J., Grilo, I.R., Oliveira, J.F., Brízida, C., Escobedo-Hinojosa, W., Cunha, I., Sobra, R.G., Vasconcelos, V., Gaudêncio, S.P., 2024. Novel metabolite madeirone and neomarinone extracted from Streptomyces aculeoletus as marine antibiofilm and antifouling agents. Front. Chem. 12 (July), 1–17. https://doi.org/10.3389/fchem.2024.1425953.

Xu, W., Xue, X., Qi, Y., Wu, N., Wang, C., 2019. Cochliomycin G , a 14-membered Resorcylic Acid Lactone from a Marine-Derived Fungus Cochliobolus Lunatus, p. 6419. https://doi.org/10.1080/14786419.2019.1633646.

Yebra, D.M., Kiil, S., Dam-Johansen, K., 2004. Antifouling technology - past, present and future steps towards efficient and environmentally friendly antifouling coatings. Prog. Org. Coating 50 (2), 75–104. https://doi.org/10.1016/j.porgcoat.2003.06.001.

Zhang, X., Smits, A.H., Van Tilburg, G.B.A., Ovaa, H., Huber, W., Vermeulen, M., 2018. Proteome-wide identification of ubiquitin interactions using UbIA-MS. Nat. Protoc. 13 (3), 530–550. https://doi.org/10.1038/nprot.2017.147.

Zhang, Y.F., Kitano, Y., Nogata, Y., Zhang, Y., Qian, P.Y., 2012. The mode of action of isocyanide in three aquatic organisms, Balanus amphitrite, bugula neritina and Danio rerio. PLoS One 7 (9), 3–9. https://doi.org/10.1371/journal.pone.0045442.

EPA United States Environmental Protection Agency, 1992. *EPA R.E.D. FACTS capsaicin*. Office of prevention. Pesticides and Toxic Substances 738 (016), 1–5.

Update

Chemosphere

Volume 369, Issue , December 2024, Page

DOI: https://doi.org/10.1016/j.chemosphere.2024.143901

Chemosphere 369 (2024) 143901

Contents lists available at ScienceDirect

Chemosphere

journal homepage: www.elsevier.com/locate/chemosphere

Corrigendum to "Antifouling activity and ecotoxicological profile of the cyanobacterial oxadiazine Nocuolin A" [Chemosphere 365 (2024), 143318]

Sandra Pereira [a,b], Isabel B. Oliveira [a], Maria Lígia Sousa [a], Catarina Gonçalves [a,b], Marco Preto [a], Maria V. Turkina [c], Vitor Vasconcelos [a,b], Alexandre Campos [a], Joana R. Almeida [a,*]

[a] CIIMAR- Interdisciplinary Centre of Marine and Environmental Research, University of Porto, Terminal de Cruzeiros do Porto de Leixões, Avenida General Norton de Matos, s/n, 4450-208, Matosinhos, Portugal
[b] Biology Department, Faculty of Sciences, University of Porto, Rua do Campo Alegre, 4169-007, Porto, Portugal
[c] Department of Biomedical and Clinical Sciences, Faculty of Medicine and Clinical Sciences, Linkoping University, 581 83, Linkoping, Sweden

GRAPHICAL ABSTRACT

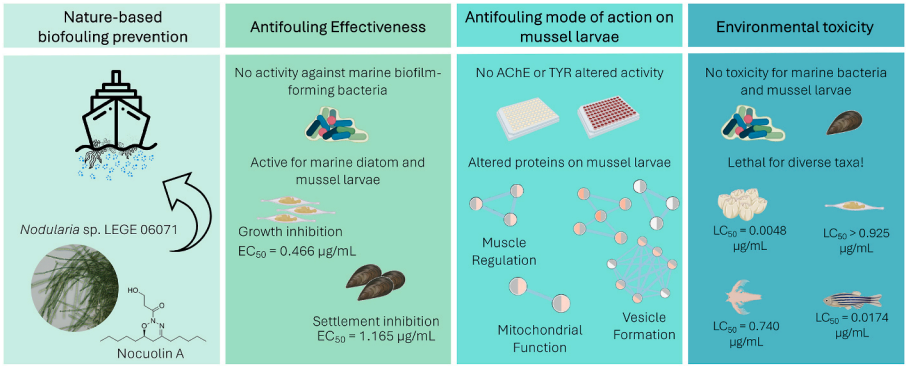

The authors regret to inform that we found an inaccuracy on the chemical structure presented in Fig. 1. Please find corrected Fig. 1 below:

The authors would like to apologise for any inconvenience caused.

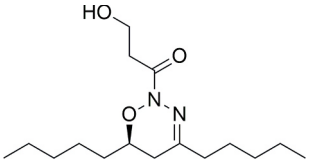

Fig. 1. Cyanobacteria-derived compound Nocuolin A.

DOI of original article: https://doi.org/10.1016/j.chemosphere.2024.143318.
* Corresponding author. CIIMAR- Interdisciplinary Centre of Marine and Environmental Research of the University of Porto Terminal de Cruzeiros do Porto de Leixões, Avenida General Norton de Matos, S/N, 4450-208, Matosinhos, Portugal.
E-mail address: jalmeida@ciimar.up.pt (J.R. Almeida).

https://doi.org/10.1016/j.chemosphere.2024.143901

Available online 7 December 2024